# Diastereoselectivity of Chloride Substitution Reactions of Cycloruthenated $(R)_C$-(+)- and $(S)_C$-(−)-Dimethyl(1-phenylethyl)amine

Saeed Attar, Vincent J. Catalano, and John H. Nelson*

*Department of Chemistry/216, University of Nevada, Reno, Nevada 89557-0020*

*Received February 1, 1996*[⊗]

The diastereoselectivity of chloride substitution in the two enantiomeric ruthenacycles ($S_{Ru}$, $R_C$)- and ($R_{Ru}$, $S_C$)-{($\eta^6$-$C_6H_6$)Ru($C_6H_4CH(Me)N(Me)_2$]} by bromide, iodide, and selected nitrogen and phosphorus donor ligands has been determined by a combination of $^1$H, $^{13}$C-{$^1$H}, and $^{31}$P{$^1$H} NMR spectroscopy, UV−visible spectroscopy, circular dichroism, and, where possible, single-crystal X-ray crystallography. The diastereoselectivity generally increases with increasing steric bulk of the incoming ligand and proceeds with predominant retention of configuration at ruthenium.



## Introduction

As recently as 1969 the first examples of the synthesis[1a] and resolution[1b] of optically active organometallic complexes containing stereogenic metal centers were reported. These were compounds of the types [($\eta^5$-$C_5H_5$)M(CO)(NO)($Ph_3P$)] (M = Cr, Mo, W) and [($\eta^5$-$C_5H_5$)Mn(CO)(NO)($Ph_3P$)]$^+PF_6^-$. The initial interest was in their utility in the resolution of racemates. It should be mentioned that in 1966 the formation of the iron(II) analogs {($\eta^5$-$C_5H_5$)Fe(CO)($Ph_3P$)[(C=O)$CH_3$]} was reported[2] in the course of an investigation of the mechanism of CO insertion into metal−carbon $\sigma$ bonds. However, the resolution of the iron compounds had not been attempted.

Soon after Brunner's initial reports,[1] his group showed that such compounds are all optically stable in the *solid* state. However, as far as their solution behavior is concerned, they may be divided into two categories: (a) those which are configurationally stable at the metal center and (b) those which are configurationally labile at the metal center. Among the examples of the first category are the diastereomeric complexes ($R_{Mn}$,$R_C$)- and ($S_{Mn}$,$R_C$)-[($\eta^5$-$C_5H_5$)Mn(CO)(NO)(L*)]$^+PF_6^-$ (L* is a chiral aminophosphine).[3ab] Reaction of these cationic complexes with LiR produces the acyl complexes ($R_{Mn}$,$R_C$)- and ($S_{Mn}$,$R_C$)-[($\eta^5$-$C_5H_5$)Mn(COR)(NO)(L*)]. These neutral acyl complexes are among examples in the second category, since they racemize (with respect to the metal stereocenter) in solution with half-lives of minutes to hours at ambient temperature.[3c,d] Thus, with compounds in the latter category, one could investigate mechanism(s) of racemization and epimerization at these chiral metal centers.[3d]

Traditionally, the stereochemistry of reaction centers has been an invaluable tool for mechanistic investigations. The configuration at the asymmetric carbon atom(s) of many organic compounds and their reaction products have been examined in detail and correlated with possible mechanism(s).[4ab] Prior to Brunner's reports,[3] such investigations on optically active organometallic and/or coordination compounds were limited to those cases where optical activity was the result of the conformation of ligands around a metal center, e.g. bis- and tris-chelate complexes of Co(III).[4c−h] Soon after Brunner established the feasibility of synthesis and resolution of optically active pseudo-tetrahedral transition-metal complexes and showed that some of them are configurationally stable in solution, it was realized that such compounds are ideally suited as stereochemical probes in mechanistic studies. This is because these saturated (18-electron) compounds are often kinetically inert to ligand dissociation under ambient conditions. In addition, their pseudo-tetrahedral geometry has two main advantages over octahedral analogs. First, chirality at the metal center is much easier to generate synthetically with only four ligands rather than six. Second, the stereochemical outcome upon changing one of the four ligands is limited to retention, inversion, or racemization, since *cis*−*trans* isomerism (present in octahedral-based systems) is not a complicating factor here. These properties were used to advantage in mechanistic studies of CO and $SO_2$ insertions into metal−carbon bonds.[5]

---

[⊗] Abstract published in *Advance ACS Abstracts,* May 15, 1996.

(1) (a) Brunner, H. *J. Organomet. Chem.* **1969**, *16*, 119. (b) Brunner, H. *Angew. Chem., Int. Ed. Engl.* **1969**, *8*, 382.

(2) Bibler, J. P.; Wojcicki, A. *Inorg. Chem.* **1966**, *5*, 889.

(3) (a) Brunner, H.; Schindler, H.-D.; Schmidt, E.; Vogel, M. *J. Organomet. Chem.* **1970**, *24*, 515. (b) *Ibid.* **1970**, *24*, C7. (c) Brunner, H.; Langer, M. *J. Organomet. Chem.* **1973**, *54*, 221. (d) Brunner, H.; Aclasis, J.; Langer, M.; Steger, W. *Angew. Chem., Int. Ed. Engl.* **1979**, *13*, 810.

(4) (a) Eliel, E. L.; Wilen, S. H. In *Stereochemistry of Organic Compounds*; Wiley: New York, 1994. (b) March, J. *Advanced Organic Chemistry*, 4th ed.; Wiley-Interscience: New York, 1992. (c) Hawkins, C. J. *Absolute Configuration of Metal Complexes*; Wiley: New York, 1971. (d) Woldbye, F. In *Technique of Inorganic Chemistry*; Jonassen, H. B., Weissberger, A., Eds.; Interscience: New York, 1965; Vol. IV, pp 249−368. (e) Saito, Y. *Inorganic Molecular Dissymmetry*; Inorganic Chemistry Concepts 4; Springer-Verlag: Berlin, 1979. (f) Mason, S. F. *Molecular Optical Activity and Chiral Discrimination*; Cambridge University Press: Cambridge, U.K., 1982; Chapter 7. (g) Sokolov, V. I. *Chirality and Optical Activity in Organometallic Compounds*; Gordon and Breach: New York, 1990. (h) Kuroda, R.; Saito, Y. In *Circular Dichroism, Principles and Applications;* VCH: Weinheim, Germany, 1994; Chapter 9.

(5) (a) Wojcicki, A. *Adv. Organomet. Chem.* **1973**, *11*, 87. (b) *Ibid.* **1974**, *12*, 31. (c) Flood, T. C.; Miles, D. L. *J. Am. Chem. Soc.* **1973**, *95*, 6460. (d) Flood, T. C.; DiSanti, F. J.; Miles, D. L. *Inorg. Chem.* **1976**, *15*, 1910. (e) Miles, S. L.; Miles, D. L.; Bau, R.; Flood, T. C. *J. Am. Chem. Soc.* **1978**, *100*, 7278. (f) Davison, A.; Martinez, N. *J. Organomet. Chem.* **1974**, *74*, C17.

S0276-7333(96)00064-7 CCC: $12.00 

During this same time period, optimization of catalysts for asymmetric hydrogenation occurred. One of the success stories of that era was the highly enantioselective (ee ≈96%) hydrogenation of the dehydroamino acid precursor to produce L-DOPA.[6a] One of the species[6b] in the catalytic cycle is a chiral rhodacycle. Following reports of that type,[6c] there was a sudden rise of interest in preparing, characterizing, and studying the reactivities of such complexes with different metal centers.[7] This interest stemmed from the rationale that catalytically active species containing metal stereocenters could undergo such simple reactions as ligand substitutions and migratory insertions. Thus, by investigation of the factors which affect the stereochemical outcome at the metal of such reactions, a better understanding of the intimate mechanism(s) of such reactions can be attained. The role that metal stereocenters could play in the course of stereoselective transformations has been discussed[6c,7a,b] and clearly demonstrated[7f] in some cases.

Despite some fruitful studies,[7] the investigation of organometallic compounds containing metal stereocenters has very much remained a topical area of research[8] as many important mechanistic questions remain open. A literature search[7,8] reveals that the majority of these investigations have concentrated on half-sandwich $\eta^5$-$C_5H_5$ complexes. The chemistry of $\eta^6$-arene analogs has been the focus of fewer studies. Among the half-sandwich complexes of the latter group, there has been a renewed interest in those containing a Ru(II) center.[8] This is due to the special stability of metal-arene bonds in these compounds.[9] In addition, studies on the kinetics of $CH_3CN/CD_3CN$ exchange equilibria in the two complexes $[(\eta^5\text{-}C_5H_5)Ru(CH_3CN)_3]^+$ and $[(\eta^6\text{-}C_6H_6)Ru(CH_3CN)_3]^{2+}$ have shown dramatic differences, indicating substantially different pathways for these two simple substitution reactions.[9d]

We recently reported[10] the synthesis and characterization of the optically stable ruthenacycles $(R_C,S_{Ru})$- and $(S_C,R_{Ru})$-$[(\eta^6\text{-}C_6H_6)RuCl(C_6H_4CH(Me)N(Me)_2]$ (**1**). In each case these ruthenacycles are a 20:1 mixture of two diastereomers((*R*$_C$,*S*$_{Ru}$)-**a** major and (*R*$_C$,*R*$_{Ru}$)-**a′** minor or (*S*$_C$,*R*$_{Ru}$)-**b′** major and (*S*$_C$,*S*$_{Ru}$)-**b** minor) so that the diastereomeric excess is 90%. This diastereomeric excess is sufficient to allow for an assessment of the stereochemistry of chloride substitution. The results of chloride substitution by bromide, iodide, and selected nitrogen and phosphorus donor ligands are described herein.

**Scheme 1**

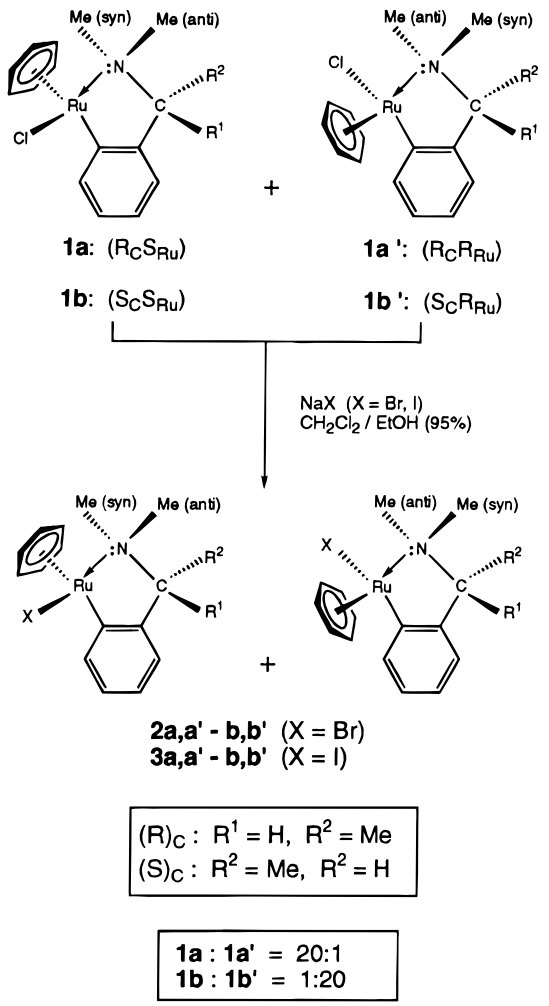


## Results and Discussion

**1. Substitution of Cl by Another Halide: Synthesis and Characterization of $\{(\eta^6\text{-}C_6H_6)RuX[C_6\text{-}H_4CH(Me)N(Me)_2]\}$ (X = Br, I).** The mixture of the chloro complexes (**1a**, **a′**; 20:1 mixture, 90% de) readily undergoes clean metathesis reactions with excess NaBr or NaI in a $CH_2Cl_2$/(95%) ETOH mixture to form the corresponding bromo (**2a**,**a′**) and iodo (**3a**,**a′**) analogs, respectively (Scheme 1), with high chemical and optical yields. These reactions are nearly stereospecific, as evidenced by the high ratios of the two diastereomers in each mixture, **2a:2a′** = 28:1 (93.2% de), and **3a:3a′** = 34:1 (94.3% de), determined by $^1$H NMR spectroscopy.[10] The $^1$H and $^{13}C\{^1H\}$ NMR spectra obtained on $CDCl_3$ solutions of each mixture are essentially the same as those of the chloro analogs[10] and do not require any further discussion.

One would expect to observe only slight shifts in the UV−visible and CD spectra of the bromo and iodo

(6) (a) Knowles, W. S.; Sabacky, M. J.; Vineyard, B. D.; Weinkauf, D. J. *J. Am. Chem. Soc.* **1975**, *97*, 2567. (b) Osborn, J. A.; Jardine, F. H.; Young, J. F.; Wilkinson, G. *J. Chem. Soc. A* **1966**, 1711. (c) Kagan, H. B. In *Comprehensive Organometallic Chemistry*; Wilkinson, G., Stone, F. G. A., Abel, E. W., Eds.; Pergamon Press: Oxford, U.K., 1982; Vol. 8, pp 463−498.

(7) (a) Brunner, H. *Acc. Chem. Res.* **1979**, *12*, 251. (b) Brunner, H. *Adv. Organomet. Chem.* **1980**, *18*, 151. (c) Faller, J. W.; Shvo, Y. *J. Am. Chem. Soc.* **1980**, *102*, 5396. (d) Quin, S.; Shaver, A.; Day, A. W. *J. Am. Chem. Soc.* **1982**, *104*, 1096. (e) Faller, J. W.; Shvo, Y.; Chao, K.; Murray, H. H. *J. Organomet. Chem.* **1982**, *226*, 251. (f) Brookhart, M.; Timmers, D.; Tucker, J. R.; Williams, G. D.; Husk, G. R.; Brunner, H.; Hammer, B. *J. Am. Chem. Soc.* **1983**, *105*, 6721. (g) Merrifield, J. H.; Fernandez, J. M.; Buhro, W. E.; Gladyz, J. A. *Inorg. Chem.* **1984**, *23*, 4022 and references cited therein. (h) Albers, M. O.; Robinson, D. J.; Singleton, E. *Coord. Chem. Rev.* **1987**, *79*, 1. (i) Consiglio, G.; Morandini, F. *Chem. Rev.* **1987**, *87*, 761. (j) Davies, S. G. *Pure Appl. Chem.* **1988**, *60*, 13. (k) Davies, S. G.; McNally, J. P.; Smallridge, A. J. *Adv. Organomet. Chem.* **1990**, *30*, 1.

(8) (a) Mandal, S. K.; Chakravarty, A. R. *J. Organomet. Chem.* **1991**, *417*, C59. (b) Mandal, S. K.; Chakravarty, A. R. *J. Chem. Soc., Dalton Trans.* **1992**, 1627. (c) Mandal, S. K.; Chakravarty, A. R. *Inorg. Chem.* **1993**, *32*, 3851. (d) Brunner, H.; Oeschey, R.; Nuber, B. *Angew. Chem., Int. Ed. Engl.* **1994**, *33*, 866. (e) Brunner, H.; Oeschey, R.; Nuber, B. *Inorg. Chem.* **1995**, *34*, 3349.

(9) (a) LeBozec, H.; Touchard, D.; Dixneuf, P. H. *Adv. Organomet. Chem.* **1989**, *8*, 2863. (b) Petrici, P.; Pitzalis, E.; Marchetti, F.; Rosini, C.; Salvadori, P.; Bennett, M. A. *J. Organomet. Chem.* **1994**, *466*, 221. (c) Faller, J. W.; Chase, K. J. *Organometallics* **1995**, *14*, 1592. (d) Luginbühl, W.; Zbinden, P.; Pittett, P. A.; Armbuster, T.; Burgi, H.-B.; Merbach, A. E.; Ludi, A. *Inorg. Chem.* **1991**, *30*, 2350.

(10) Attar, S.; Nelson, J. H.; Fischer, J.; DeCian, A.; Sutter, J.-P.; Pfeffer, M. *Organometallics* **1995**, *14*, 4559.

analogs compared to those of the chloro compound, as is indeed the case. Each UV−visible ($CH_2Cl_2$) spectrum displays two absorption maxima with similar absorptivities ($\lambda_{max}$ (nm) ($\epsilon$ (L mol$^{-1}$ cm$^{-1}$))): **1a,a′** (X = Cl), 378 (1.7 × 10$^3$), 440 (1.5 × 10$^3$); **2a,a′** (X = Br), 380 (1.7 × 10$^3$), 448 (1.4 × 10$^3$); **3a,a′** (X = I), 382 (1.2 × 10$^3$), 472 (1.0 × 10$^3$)). Both the signs and morphologies of the CD spectra of the three compounds are also very similar, suggesting that the absolute configurations of the major species in solution are the same.[5,7b,8] The absolute configuration at the Ru center of the major diastereomer of the chloro complex has been established previously as $S_{Ru}$.[10] Since these diastereomers are configurationally stable and the chirality at the benzylic carbon atom of **1a,a′** remains $R_C$ during the course of these substitution reactions, we assign to both **2a** and **3a** an $S_{Ru},R_C$ and to both **2a′** and **3a′** an $R_{Ru},R_C$ absolute configuration as the major and minor diastereomers, respectively. Both assignments of Ru absolute configurations are opposite to their *formal* designations of $R_{Ru}$ and $S_{Ru}$, respectively (*vide infra*). These results are similar to those reported[11] for the halide exchange reactions of [($\eta^5$-$C_5H_4$R*)Ru(CO)($Ph_3$P)(X)] (R* = menthyl, neomenthyl; X = Cl, Br, I).

The above conclusions on the ruthenium absolute configurations in **2a,a′** and **3a,a′** (and hence the stereochemistry of the reactions leading to their formation) were confirmed by the crystal structure of **3a**, the major diastereomer (Figure 1a). The structure consists of isolated molecules with no unusual intermolecular contacts. The structure suffers from a positional disorder (Figure 1b). The structures of **1b′**[10] and **3a** are similar. The two metrical parameters worthy of note are the Ru−X distances (**1b′** (X = Cl), 2.439(1) Å; **3a** (X = I), 2.772(10) Å) and the Ru−N distances (**1b′**, 2.193(3) Å; **3a**, 2.118(11) Å), both reflecting the effect of the increased steric bulk of iodide relative to chloride. The Ru−I distance is slightly longer than that observed[11] (2.708(1) Å) for [($\eta^5$-$C_5H_4$R*)Ru(CO)($Ph_3$P)(I)] (R* = neomenthyl). The Ru−N distance in **3a** is very close to the estimated value of 2.12 Å based on a Ru covalent radius of 1.42 Å[12a] and a N(sp$^3$) radius of 0.70 Å.[12b] The Ru−C(aryl) distance (2.095(3) Å) is slightly longer than that in **1b′** (2.057(3) Å); this may be due to the greater *trans* influence[13] of I compared to that of Cl. The five-membered chelate ring again adopts a conformation wherein the benzylic C−$CH_3$ group is nearly in the plane of the aryl ring.[14]

The most significant aspect of this structural determination is the unequivocal assignment of absolute configuration of the Ru center of **1a**. We concluded, on the basis of CD spectroscopy, that the configuration is $S_{Ru}$. However, on the basis of the arrangement of ligands around the Ru atom in **1a**, formally an $R_{Ru}$ configuration is assigned from the crystal structure data. The change in the *formal* designation of configuration merely arises from a change in the position of the halide atom in the ligand priority sequence,[15] where the ligand priority is $\eta^6$-$C_6H_6$ (1) > Cl (2) > N (3) > C(aryl) (4) but I (1) > $\eta^6$-$C_6H_6$ (2) > N (3) > C (aryl) (4). A comparison of the structures of **3a** and **1b′** shows that the absolute stereochemical arrangements of the ligands (atoms) around the Ru centers in both compounds are the same. Since both **2a** and **3a** are configurationally stable in solution for days, as was observed for **1b′**,[10] these two chloride substitution reactions proceed with predominant retention of configuration at ruthenium for the major diastereomer. In the bromide reaction 32%

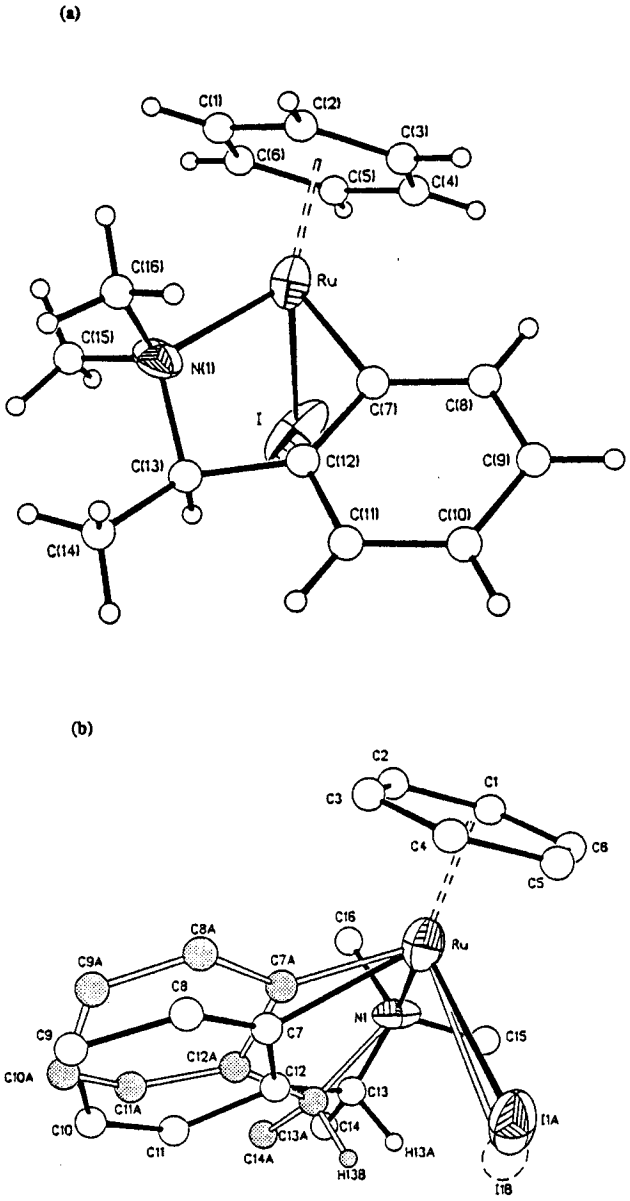


**Figure 1.** (a) Structural drawing of **1a**, showing the atom-numbering scheme (50% probability ellipsoids; hydrogen atoms have an arbitratry radius of 0.1 Å). Selected bond lengths (Å) and angles (deg): Ru−C(aryl), 2.095(3); Ru−C(arene, av), 2.181(11); Ru−I, 2.772(10); Ru−N, 2.118(11); C(aryl)−Ru−N, 78.6(8); C(aryl)−Ru−I, 88.5(7); N−Ru−I, 90.4(3). (b) Structural drawing of **1a**, showing the positional disorder of this molecule.

(11) Cesarotti, E.; Chiesa, A.; Ciani, G. F.; Sironi, A.; Vefghi, R.; White, C. *J. Chem. Soc., Dalton Trans.* **1984**, 653.

(12) (a) Howard, J.; Woodward, P. J. *J. Chem. Soc., Dalton Trans.* **1975**, 59. (b) Bennett, M. J.; Mason, R. *Nature* **1965**, *205*, 760.

(13) Appleton, T. G.; Clark, H. C.; Manzer, L. E. *Coord. Chem. Rev.* **1973**, *10*, 335.

(14) (a) Van der Schaaf, P. A.; Boersma, J.; Kooijman, H.; Spek, A. L.; Van Koten, G. *Organometallics* **1993**, *12*, 4334. (b) Alcock, N. W.; Hulmes, D. I.; Brown, J. M. *J. Chem. Soc., Chem. Commun.* **1995**, *395*. (c) Jiang, Q.; Rüegger, H.; Venanzi, L. M. *J. Organomet. Chem.* **1995**, *488*, 233. The first two citations claim that this conformation is rare, whereas the third claims that it is found approximately 50% of the time for such rings.

(15) (a) Stanley, K.; Baird, M. C. *J. Am. Chem. Soc.* **1975**, *97*, 6598. (b) Cahn, R. S.; Ingold, C.; Prelog. V. *Angew. Chem., Int. Ed. Engl.* **1966**, *5*, 385.

of the minor diastereomer undergoes inversion and in the iodide reaction 43% of the minor diastereomer undergoes inversion.

**2. Substitution of Cl by Phosphines: Synthesis and Characterization of {($\eta^6$-$C_6H_6$)Ru[$C_6H_4$CH(Me)N(Me)$_2$]($R_3P$)}$^+X^-$ ($X^-$ = $PF_6$, $BF_4$, $BPh_4$). A. $R_3P$ = $Ph_3P$.** In a polar solvent mixture, and in the presence of a chloride scavenger such as $NaPF_6$ or $NaBPh_4$, the chloro complexes **1a**,**a′** and **1b**,**b′** undergo a substitution reaction with $Ph_3P$ to produce mixtures of the diastereomeric complexes **4a**,**a′**−**4b**,**b′** ($X^-$ = $PF_6$) or **5a**,**a′**−**5b**,**b′** ($X^-$ = $BPh_4$). However, when these reactions were carried out with $Ag(F_3CSO_3)$ or $AgBF_4$ as the chloride scavenger, the presence of Ag(I) seemed to promote redox reactions.

The progress of the substitution reaction was monitored by $^{31}P\{^1H\}$ NMR spectroscopy. The spectrum of a $CDCl_3$ solution, immediately after equimolar amounts of **1b**,**b′** (1:20), $Ph_3P$, and $NaPF_6$ (dissolved in 2 drops of $D_2O$) were mixed, exhibited the singlet resonances $\delta$ 32.9, 31.2, 28.8, 26.3, and −6.0 (due to free $Ph_3P$) in a 1:3.5:1.1:1.0 ratio as well as the septet due to $PF_6^-$ ($\delta$ −144.7). The two downfield resonances ($\delta$ 32.9, 31.2; ratio 1:1.7) are attributed to the two expected diastereomeric cations ($S_{Ru}$,$S_C$)- and ($R_{Ru}$,$S_C$)-{($\eta^6$-$C_6H_6$)Ru[$C_6H_4$CH(Me)N(Me)$_2$]($Ph_3P$)}$^+$ $PF_6^-$ (**4b** and **4b′**, respectively; *vide infra*). The resonance at $\delta$ 28.8 is attributed to $Ph_3P$=O, but the origin of the resonance at $\delta$ 26.3 is not clear. The original orange-red color of this solution became dark green on overnight standing (∼15 h) at ambient temperature. The $^{31}P\{^1H\}$ NMR spectrum of this solution showed an increase in the intensities of the four downfield resonances, while that due to free $Ph_3P$ disappeared. In addition, the ratio of the intensities of the two resonances assigned to **4b** ($\delta$ 32.9) and **4b′** ($\delta$ 31.2) increased from 1:1.7 to 1:4.3 during this time period. After 3 days no further changes were observed in the $^{31}P\{^1H\}$ NMR spectrum of this dark green solution. Thus, it is concluded that **4b** and **4b′** form at different rates and that **4b** and **4b′** are configurationally stable. This latter conclusion is supported by the time independence of the $^1H$ and $^{13}C\{^1H\}$ NMR and CD spectra of these complexes.

When this reaction was carried out on a larger scale, after initial work up (removal of insoluble salts and solvent then washing with ether/hexane), the crude reaction product (an orange-yellow solid) showed three resonances at $\delta$ 33.0, 31.2, and −144.7 ppm in a 1:4:5 ratio in its $^{31}P\{^1H\}$ NMR ($CDCl_3$) spectrum. This ratio is comparable to that obtained for **4b** and **4b′** in the "NMR tube" experiment. Since these two complexes are configurationally stable, the diastereomeric excess (de) of this reaction is 60% (80% major, **4b′**; 20% minor, **4b**).

The absolute configuration at the Ru center was determined on a sample whose $^{31}P\{^1H\}$ NMR spectrum showed resonances at $\delta$ 31.2 and −144.7 ppm in a 1:1 ratio (major diastereomer, **4b′**). The structures of the two independent cations are shown in Figure 2. The absolute configuration at the Ru atom of each cation is assigned[15] as $R_{Ru}$. Thus, the configuration is $R_{Ru}$,$S_C$ for the major diastereomer.

The Ru−P distances (2.392(3), 2.362(3) Å) are comparable to those reported[8d] (2.392(4), 2.355(4) Å) for the two "propeller isomers" of ($R_{Ru}$,$S_C$)-{($\eta^6$-$C_6H_6$)Ru[*o*-$C_6H_4$CH=NCH(Me)Ph]($Ph_3P$)}$^+PF_6^-$. Of the two possible[4a] enantiomeric conformations of the $Ph_3P$ ligand, M and P, the former is present in both cations. The conformation of the five-membered chelate ring[14] is the same as those found for the starting chloro complex **1b′** and the iodo complex **3a**.

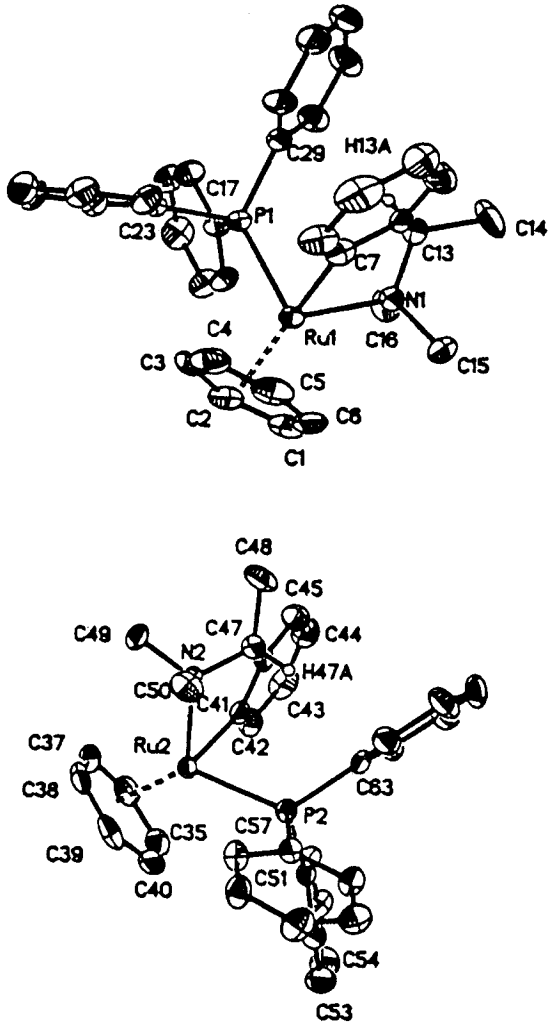


**Figure 2.** Structural drawing of the two independent cations of **4b′**, showing the atom-numbering scheme (50% probability ellipsoids; the benzylic hydrogen atoms (H13A and H47A) have an arbitrary radius of 0.1 Å). Selected bond lengths (Å) and angles (deg) for cations 1 and 2, respectively: Ru−C(aryl), 2.081(11), 2.096(10); Ru−C(arene, av), 2.250(12), 2.253(11); Ru−N, 2.191(9), 2.211(9); Ru−P, 2.392(3), 2.362(3); C(aryl)−Ru−N, 77.6(4), 77.3(4); C(aryl)−Ru−P, 86.4(3), 86.5(3); N−Ru−P, 95.7(3), 97.3(3).

The UV−visible ($CH_2Cl_2$) spectrum of **4b′** shows two strong absorption maxima ($\lambda_{max}$, nm ($\epsilon$, L mol$^{-1}$ cm$^{-1}$): 326 ($2.7 \times 10^3$), 400 ($1.7 \times 10^3$)). The CD spectrum of the same solution shows a single positive Cotton effect centered around 356 nm. Both the sign and shape of this Cotton effect compare well with those of the Cotton effect exhibited by **1b′** at 368 nm, consistent with the conclusion that both species have the $R_{Ru}$,$S_C$ absolute configuration. Thus, this $Ph_3P$ substitution reaction proceeds predominantly with retention of configuration at ruthenium.

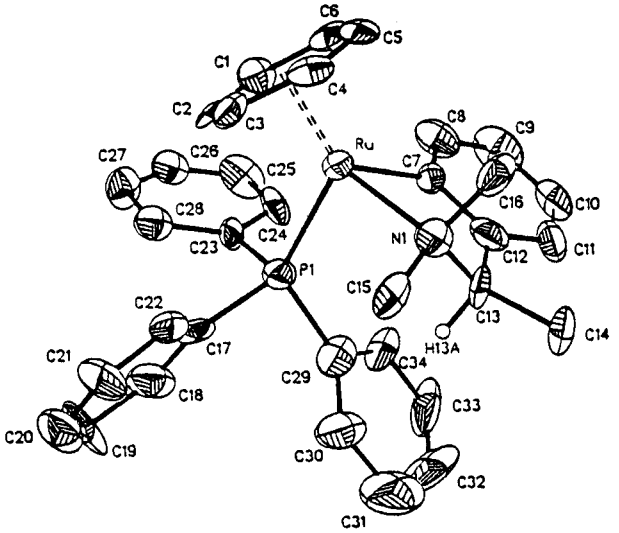


**Figure 3.** Structural drawing of the cation of **5a**, showing the atom-numbering scheme (50% probability ellipsoids; the benzylic hydrogen atom (H13A) has an arbitrary radius of 0.1 Å). Selected bond lengths (Å) and angles (deg): Ru−C(aryl), 2.07(2); Ru−C(arene, av), 2.255(6); Ru−N, 2.199(12); Ru−P, 2.357(5); C(aryl)−Ru−N, 77.3(7); C(aryl)−Ru−P, 85.6(4); N−Ru−P, 95.5(3).

When the above reaction was carried out with a **1a**,**a′** diastereomeric mixture (**1a**:**1a′** = 20:1; $S_{Ru}R_C$ major species) and the Cl scavenger was changed from $NaPF_6$ to $NaBPh_4$, the resulting **5a**,**a′** product mixture exhibited two resonances ($\delta$ 31.4, 32.8) in a 3.3:1 ratio in its $^{31}P\{^1H\}$ NMR ($CDCl_3$) spectrum. The chemical shifts and the diastereoselectivity are only slightly different from those obtained for the **4b**,**b′** mixture described above. Dropwise addition of a 1:1 ether/hexane mixture to this orange-red $CDCl_3$ solution, and gradual diffusion of the solvents, produced orange-red crystals. The $^{31}P\{^1H\}$ NMR spectrum of a $CDCl_3$ solution of these crystals showed a single resonance at $\delta$ 31.4 (the major species, **5a**).

The crystal structure of **5a** (Figure 3) shows that this cation has an $S_{Ru}R_C$ absolute configuration, indicating predominant retention of configuration at ruthenium. The bond distances and angles, as expected, are similar to those found for **4b′** (Figure 2). The conformation of the $Ph_3P$ ligand is assigned[4a] as P, enantiomeric to that found in **4b′**.

The UV−visible ($CH_2Cl_2$) spectrum of **5a** is identical with that of **4b′**. Hence, the change in the counterion from $PF_6^-$ in **4b′** to $BPh_4^-$ in **5a**, as expected, does not cause any shifts in the positions of the absorption maxima in the 300−600 nm region. The CD spectrum of **5a** shows a single negative Cotton effect centered around 356 nm. This is comparable in its sign and shape to the Cotton effect at 368 nm exhibited by the starting chloro compound **1a**. Thus, both major species **5a** and **1a**, having an $S_{Ru}R_C$ absolute configuration, show a similarly shaped, negative Cotton effect at about 360 nm. The CD spectra of **4b′** and **5a** show an enantiomeric relationship (Figure 4), as expected, since the Ru absolute configuration in **4b′** ($R_{Ru}$) is opposite to that in **5a** ($S_{Ru}$).

**B. $R_3P$ = 1-Phenyldibenzophosphole (DBP).** 1-Phenyldibenzophosphole (DBP) is a cyclic analog of $Ph_3P$. The structural chemistry of this ligand with a variety of transition metals has been the subject of several investigations.[16] Through such studies it has become clear that although DBP has $\sigma$-donor and $\pi$-acceptor properties that are similar to those of $Ph_3P$, its smaller steric requirements make it possible to isolate complexes with unusual structures.[16a]

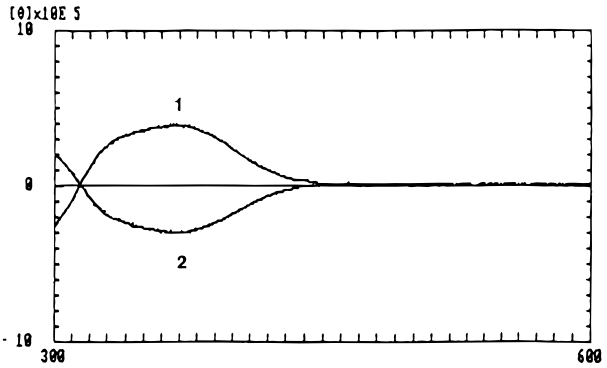


**Figure 4.** CD spectra of **4b,b′** (60% de, curve 1) and **5a,a′** (53.5% de, curve 2) in $CH_2Cl_2$ ($1.1 \times 10^{-4}$ M, 1 cm path length cell), showing their enantiomeric relationship.

As in the case of $Ph_3P$, the progress of the DBP substitutions of chloride in **1a**,**a′** was monitored by $^{31}P\{^1H\}$ NMR spectroscopy. When equimolar amounts of **1a**,**a′** (20:1 ratio), DBP, and $NaPF_6$ (dissolved in 2 drops of $D_2O$) were mixed with $CDCl_3$, a yellow solid formed rapidly. After filtration, the resulting transparent orange-mustard $CDCl_3$ solution showed the following singlet resonances (in addition to the septet centered at $\delta$ −145.0 due to $PF_6^-$) in its $^{31}P\{^1H\}$ NMR spectrum: $\delta$ 33.2, 29.4, 28.7, 12.0, −8.7 (broad) in the following ratios: 1:3.2:1.6:1.9:1.1. The resonance at $\delta$ 33.2 is assigned to DBP═O. The resonances at $\delta$ 29.4 and 28.7 (2:1 ratio) are assigned to the expected products of DBP substitution, **6a**,**a′**, ($S_{Ru}$,$R_C$)- and ($R_{Ru}$,$R_C$)-{($\eta^6$-$C_6H_6$)-Ru[$C_6H_4$CH(Me)N(Me)$_2$](DBP)}$^+$ $PF_6^-$ (**6a**,**a′**, respectively. The origin of the resonance at $\delta$ 12.0 is not clear, but the broad resonance at $\delta$ −8.7 may be assigned to free DBP. The breadth of this resonance and its chemical shift change from free DBP ($\delta$ −10.6 ppm) suggest an underlying exchange process. Extraction of the yellow solid that formed initially with $CDCl_3$ gave a transparent greenish yellow solution that exhibited the $^{31}P\{^1H\}$ resonances $\delta$ 33.2, 29.3, 29.1, 28.7, 27.8 in the ratio 1:2.8:1.4:1.9:1.6. When this solution stood overnight (∼15 h) at ambient temperature, the color of this solution did not change appreciably (as it does in the $Ph_3P$ case); the $^{31}P\{^1H\}$ NMR spectrum of this solution also did not change. The resonances at $\delta$ 33.2, 29.3, and 29.1 are assigned to DBP═O and **6a**,**a′**; the origins of the resonances at $\delta$ 28.7 and 27.8 remain unclear.

(16) (a) Attar, S.; Bearden, W. H.; Alcock, N. W.; Alyea, E. C.; Nelson, J. H. *Inorg. Chem.* **1990**, *29*, 425 and references cited therein. (b) Nelson, J. H.; Mathey, F. In *Phosphorus-31 NMR Spectroscopy in Stereochemical Analysis*; Verkade, J. G., Quin, L. D., Eds.; VCH: Deerfield Beach, FL, 1987; pp 665−694. (c) Mathey, F.; Fischer, J.; Nelson, J. H. *Struct. Bonding (Berlin)* **1983**, *55*, 153. (d) Kessler, J. M.; Reeder, J.; Vac, R.; Yeung, C.; Nelson, J. H.; Frye, J. S.; Alcock, N. W. *Magn. Reson. Chem.* **1991**, *29*, S94. (e) Attar, S.; Alcock, N. W.; Bowmaker, G. A.; Frye, J. S.; Bearden, W. H.; Nelson, J. H. *Inorg. Chem.* **1991**, *30*, 4166. (f) Alyea, E. C.; Malito, J.; Attar, S.; Nelson, J. H. *Polyhedron* **1992**, *11*, 2409. (g) Kessler, J. M.; Nelson, J. H.; Frye, J. S.; DeCian, A.; Fischer, J. *Inorg. Chem.* **1993**, *32*, 1048. (h) Bowmaker, G. A.; Clase, H. J.; Alcock, N. W.; Kessler, J. M.; Nelson, J. H.; Frye, J. S. *Inorg. Chim. Acta* **1993**, *210*, 107. (i) Holah, D. G.; Hughes, A. N.; Wright, K. *Coord. Chem. Rev.* **1975**, *15*, 239.

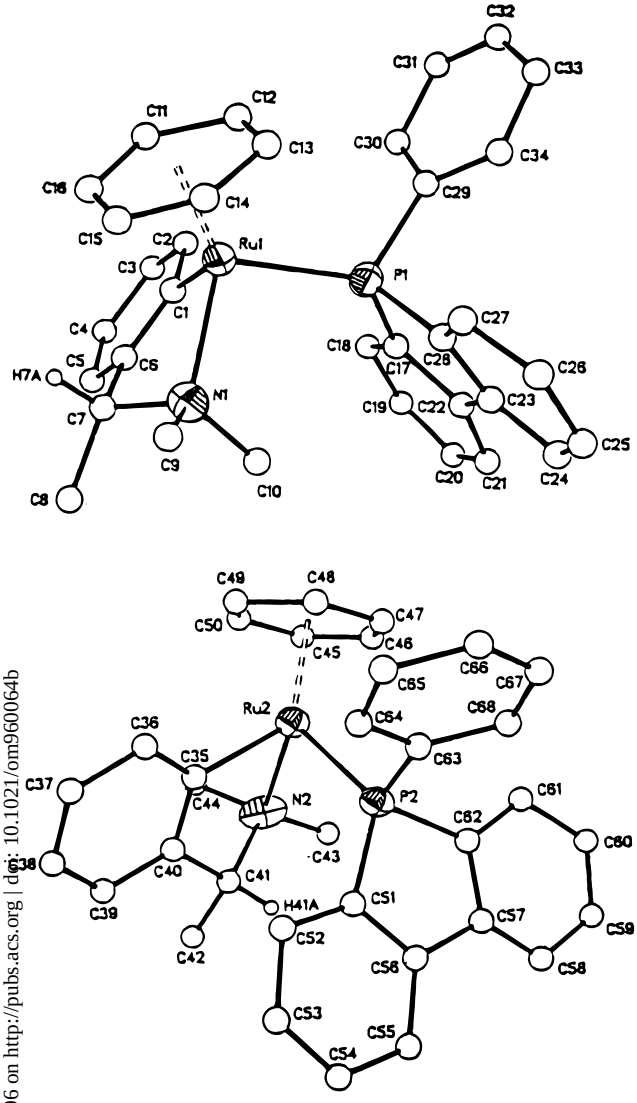





**Figure 5.** Structural drawings of the two diastereomeric cations **6a′** (top) and **6a** (bottom), showing the atom-numbering scheme (50% probability ellipsoids; the benzylic hydrogen atoms (H7A and H41A) have an arbitrary radius of 0.1 Å). Selected bond lengths (Å) and angles (deg) for **6a′** and **6a**, respectively: Ru−C(aryl), 2.04(2), 2.10 (3); Ru−C(arene, av), 2.22(3), 2.27(3); Ru−N, 2.23(2), 2.21(2); RuP, 2.315(7), 2.343(7); C(aryl)−Ru−N, 76.4(9), 79.1(9); C(aryl)−Ru−P, 94.0(6), 85.5(6); N−Ru−P, 95.3(5), 96.4(5).

When the above reaction was performed on a larger scale and with $CH_3CN$ as the solvent, a green-mustard solid was obtained. Addition of $CH_2Cl_2$ to the solid, followed by filtration, gave a faint yellowish green solution. Addition of $CH_3OH$ and ether/hexane (1:1) with gradual diffusion of the solvents resulted in the formation of a small quantity of orange-red, wedge-shaped crystals. The $^{31}P\{^1H\}$ NMR ($CDCl_3$) spectrum of these crystals showed three resonances: $\delta$ 29.4, 28.6 and −145.0 in a 2:1:3 ratio. The spectrum was unchanged after 3 days at ambient temperature. Thus, **6a**,**a′** are also configurationally stable.

An X-ray crystallographic study, performed on a suitable single crystal from the above sample, showed the presence of two independent cations (Figure 5) in the unit cell with opposite configurations at ruthenium. Cations **6a′** and **6a** have $R_{Ru},R_C$ and $S_{Ru},R_C$ absolute configurations, respectively. The metrical parameters for the two diastereomers are similar. However, the

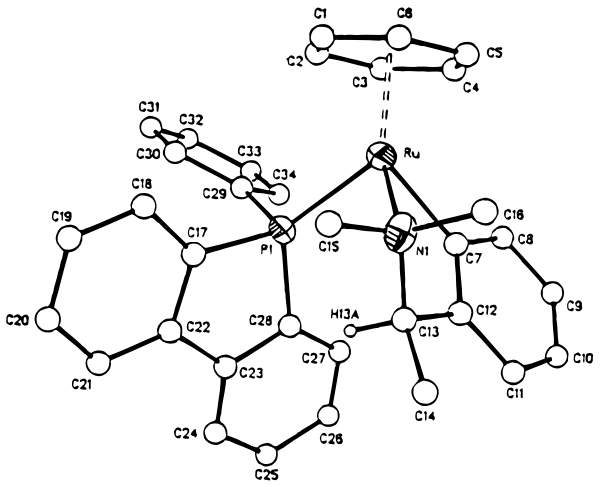


**Figure 6.** Structural drawing of the cation of **6a**, showing the atom-numbering scheme (50% probability ellipsoids; the benzylic hydrogen atom (H13A) has an arbitrary radius of 0.1 Å). Selected bond lengths (Å) and angles (deg): Ru−C(aryl), 2.102(9); Ru−C(arene, av), 2.26(3); Ru−N, 2.165(9); Ru−P, 2.327(7); C(aryl)−Ru−N, 76.4(4); C(aryl)−Ru−P, 86.4(5); N−Ru−P, 94.8(3).

Ru(1)−P(1) bond length in **6a′** (2.315(7) Å) is slightly shorter than the Ru(2)−P(2) bond length in **6a** (2.343(7) Å). At this point we cannot ascertain which of these two species is the major product.

When the above crystalline sample of **6a,a′** was washed with $CH_3OH$ (0.5 mL) and $CDCl_3$ (2.5 mL) and the washings were left standing at ambient temperature for 2 weeks, another crystalline sample (very small) was formed. The $^{31}P\{^1H\}$ NMR ($CDCl_3$) spectrum showed the two resonances $\delta$ 29.4 and −145.0 in a 1:1 ratio corresponding to the major diastereomer. An X-ray crystallographic study, performed on a suitable single crystal from this sample, showed the cation (Figure 6) to have the $S_{Ru},R_C$ absolute configuration. Since the absolute configurations at the Ru atoms of both **6a** and **1a** are the same, we conclude that the DBP substitution reaction also proceeds with predominant retention of configuration at Ru.

The structure of **6a** consists of isolated cations and anions with no unusual interionic contacts. The environment around Ru(II) in this cation is very similar to those previously described for the $Ph_3P$ analogs **4b′** and **5a**. It is noteworthy that the Ru-P bond lengths in the DBP-substituted compounds (**6a**, 2.327(7) and 2.343(7) Å; **6a′**, 2.315(7) Å) are slightly shorter than those in the $Ph_3P$-substituted analogs (**4b′**, 2.362(3) and 2.392(3) Å; **5a**, 2.357(5) Å). This may suggest a slightly better $\sigma$-donor ability of DBP towards Ru(II) as compared to that of $Ph_3P$. DBP also seems to be a better $\sigma$ donor toward Rh(I).[16g]

The UV−visible ($CH_2Cl_2$) spectrum of **6a** shows two strong absorption maxima ($\lambda_{max}$, nm ($\epsilon$, L mol$^{-1}$ cm$^{-1}$): 318 ($4.5 \times 10^3$), 403 ($1.7 \times 10^3$)). This is similar to the UV−visible spectra of both $Ph_3P$ analogs, **4b′** and **5a** (326 ($2.7 \times 10^3$), 400 ($1.7 \times 10^3$)), except that the band at 326 nm for the latter compounds has undergone a hypsochromic shift to 318 nm for **6a** in addition to an increase in intensity. The CD spectrum of the same $CH_2Cl_2$ solution of **6a** shows two negative Cotton effects, a broad one at about 370 nm and a narrower one at about 337 nm. The former compares well with the negative Cotton effect at 368 nm in the CD spectrum of

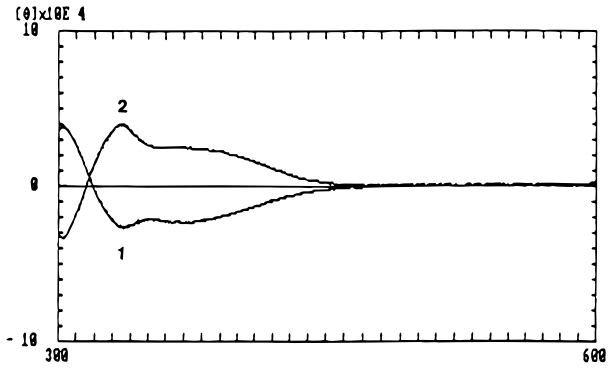


**Figure 7.** CD spectra of **6a,a′** (33.3% de, curve 1) and **7b,b′** (33.3% de, curve 2) in $CH_2Cl_2$ ($1.1 \times 10^{-4}$ M, 1 cm pathlength cell), showing their enantiomeric relationship.

the starting chloro complex mixture **1a,a′,** where the major species (**1a**) has an $S_{Ru}$ configuration.

Once again, the sign of the shorter wavelength Cotton effect is indicative of the absolute configuration at Ru.

When the above reaction was carried out with a **1b,b′** (1:20) starting mixture, $NaBPh_4$ as the halide scavenger, and $CH_2Cl_2$/acetone as the solvent mixture, an orange-mustard solid was initially obtained. The $^{31}P\{^1H\}$ NMR spectrum of a $CDCl_3$ solution of this solid showed the following resonances: $\delta$ 33.2, 29.4, 29.2, and −10.6. The downfield resonance at $\delta$ 33.2 may be assigned to DBP═O and the upfield one at $\delta$ −10.6 to free DBP. The two resonances at $\delta$ 29.4 and 29.2 (2:1 ratio) may be assigned to the two diastereomers expected in this reaction, ($R_{Ru},S_C$)- and ($S_{Ru},S_C$)-{($\eta^6$-$C_6H_6$)Ru[$C_6H_4$CH(Me)N($Me)_2$](DBP)}$^+BPh_4^-$ (**7b** and **7b′**, respectively). The diastereoselectivity of this reaction then (2:1 ratio, 33.3% de) is the same as what was observed for the $PF_6^-$ analog **6a,a′**.

When this initial product mixture was washed thoroughly with ether (to remove excess DBP) and crystallized from a $CH_2Cl_2$/ether−hexane (1:1) mixture, the resulting orange-mustard, flaky needles showed the same two $^{31}P$ resonances ($\delta$ 29.4, 29.2) in the same ratio (2:1) in its $^{31}P\{^1H\}$ NMR ($CDCl_3$) spectrum.

As would be expected, the UV−visible ($CH_2Cl_2$) spectrum of **7b,b′** is identical with that of **6a,a′**. However, the CD spectra ($CH_2Cl_2$) of **7b,b′** and **6a,a′** (Figure 7) show an enantiomeric relationship. Since the absolute configuration of **6a** has been established as $S_{Ru},R_C$, that of the major diastereomer in the **7b,b′** mixture (i.e. **7b′**) may be assigned as $R_{Ru},S_C$.

**C. $R_3P$ = 1-Phenyl-3,4-dimethylphosphole (DMPP).** 1-Phenyl-3,4-dimethylphosphole (DMPP), like DBP, is a member of the family of phospholes with similar $\sigma$-donor properties toward transition metals.[16b,c] This ligand, however, is sterically much less demanding than either DBP or $Ph_3P$. In addition, DMPP contains two "localized" double bonds, which increase the number of ways that it can coordinate to a metal center.[16c] The latter "unsaturated" C−C bonds may also have the potential to insert into the Ru-C bonds of the starting materials **1a,a′,b′b′**.[17]

An attempt to monitor the DMPP substitution of Cl in **1a,a′** *via* a $^{31}P$ NMR tube experiment was complicated by the factors mentioned above. When equimolar amounts of **1a,a′**, DMPP, and $NaPF_6$ (on $D_2O$) were mixed with $CDCl_3$ in a 10- mm NMR tube, the $^{31}P\{^1H\}$ NMR spectrum of the resulting dark orange-mustard solution indicated, in addition to the $PF_6^-$ resonance, the presence of at least 10 species! The assignments of these resonances, except for those of DMPP,[16c] [DMPP═O]$_2$,[16c] and the two expected substitution products, are not easily accomplished. When it stood at ambient temperature, the above $CDCl_3$ solution turned dark green within 3 h. The $^{31}P\{^1H\}$ NMR spectrum was essentially invariant over a 2-day period.

When the above reaction was carried out on a larger scale with $NaBPh_4$ as the Cl scavenger, a yellow-orange solid was obtained. The $^{31}P\{^1H\}$ NMR ($CDCl_3$) spectrum of this solid showed three singlet resonances at $\delta$ 42.6, 41.1, and 34.8 in a 1.3:1:3.2 ratio. By comparison with the data for the $Ph_3P$ and DBP analogs, the two downfield resonances were assigned to the two expected diastereomers **8a** and **8a′**, ($S_{Ru},R_C$)- and ($R_{Ru},R_C$)-{($\eta^6$-$C_6H_6$)Ru[$C_6H_4$CH(Me)N($Me)_2$](DMPP)}$^+BPh_4^-$, respectively. The origin of the resonance at $\delta$ 34.8 remains unclear. From the 1.3:1 diastereomeric ratio, the stereoselectivity of this reaction is calculated as 13.0% de.

All attempts to obtain a pure crystalline sample met with failure. The stereochemistry of this reaction, however, may be inferred from the CD spectrum ($CH_2Cl_2$) of the crude mixture. The UV−visible ($CH_2Cl_2$) spectrum of this sample shows two strong absorption maxima ($\lambda_{max}$, nm ($\epsilon$, L mol$^{-1}$ cm$^{-1}$): 325 ($3.2 \times 10^3$), 406 ($1.1 \times 10^3$)), which resemble those of the DBP and $Ph_3P$ analogs. The CD spectrum of this sample shows a broad, negative Cotton effect at 382 nm, which is comparable to the Cotton effect exhibited by the starting **1a,a′** mixture in its CD spectrum. On the basis of the earlier arguments regarding the correlation between the sign of this shorter wavelength Cotton effect and the Ru absolute configuration, we assign an overall $S_{Ru},R_C$ configuration to the major species in the **8a,a′** mixture (i.e. **8a**). The low magnitude of the negative Cotton effect at 382 nm for this mixture is a result of the low diastereoselectivity (13% de). Thus, we conclude that the DMPP substitution proceeds with predominant retention of configuration at Ru.

**D. $R_3P$ = $Et_3P$.** Reaction of equimolar quantities of **1b,b′**, $Et_3P$, and $NaBPh_4$ in a $CH_2Cl_2$/$CH_3OH$ solution afforded a golden green solid. The $^{31}P\{^1H\}$ NMR ($CDCl_3$) spectrum of this solid showed two resonances ($\delta$ 19.4 and 17.2) in a 1:1.7 ratio (25.9% de). These resonances are assigned to the two expected diastereomers **9b** and **9b′**, ($S_{Ru},S_C$)- and ($R_{Ru},S_C$)-{($\eta^6$-$C_6H_6$)Ru[$C_6H_4$CH(Me)N($Me)_2$]($Et_3P$)}$^+BPh_4^-$.

The UV−visible ($CH_2Cl_2$) spectrum of the **9b,b′** mixture shows two strong absorption maxima ($\lambda_{max}$, nm ($\epsilon$, L mol$^{-1}$ cm$^{-1}$): 328 ($2.7 \times 10^3$), 408 ($1.9 \times 10^3$)). The CD spectrum ($CH_2Cl_2$) of this mixture shows two weak Cotton effects: a negative one at 430 nm and a positive one at about 366 nm. This compares with the CD spectrum of the **1b,b′** mixture, which shows a negative Cotton effect at 462 nm and a positive one at 369 nm. On the basis of the arguments presented previously, we assign to the major diastereomer in this mixture, **9b′**, the $R_{Ru},S_C$ absolute configuration and conclude that this

(17) (a) Abbenhuis, H. C. L.; Pfeffer, M.; Sutter, J.-P.; DeCian, A.; Fischer, J.; Ji, H. -L.; Nelson, J. H. *Organometallics* **1993**, *12*, 4464. (b) Pfeffer, M. *Pure Appl. Chem.* **1992**, *64*, 335.

substitution reaction proceeds with predominant retention of configuration at Ru.

**E. $R_3P$ = 1,3,4-Triphenyl-1,2-dihydrophosphete (TPHP).** 1,3,4-Triphenyl-1,2-dihydrophosphete (TPHP) is a chiral phosphorus ligand with good donor properties.[18] In order to ascertain whether the ruthenacycles **1a,a′** might be useful in resolving racemic mixtures of chiral phosphines, we reacted equimolar amounts of **1a,a′**, TPHP, and $NaPF_6$ in $CH_2Cl_2/CH_3OH$. After workup in the usual manner, an orange-mustard solid was obtained. The $^{31}P\{^1H\}$ ($CDCl_3$) spectrum of this solid showed four singlet resonances ($\delta$ 64.4, 61.1, 59.4, 53.2, in addition to the septet centered at $\delta$ −145.0 ppm) in the ratio 1.4:1:1.7:1.4. These may be assigned to the four diastereomers (each with three chiral centers now) expected in this reaction: $S_{Ru},R_C,R_P$, $R_{Ru},R_C,R_P$, $S_{Ru},R_C,S_P$, and $R_{Ru},R_C,S_P$. The ratios of these species in solution suggest that the stereoselectivity of this reaction, and hence the asymmetric induction by **1a,a′,** is poor. Because of this fact and also because these species decompose in solution within hours at ambient temperature, this reaction was not pursued further.

**F. $R_3P$ = 1,2-Bis(diphenylphosphino)ethane (dppe).** In order to ascertain whether a potentially chelating phosphine could displace chloride and also stabilize the Ru−N bond, we have studied the reaction of dppe with the ruthenacycles **1a,a′**. Our premise was that if the diphosphine did not open up the C−N chelate ring, this would add further support for our contention that the ruthenacycles do not epimerize by such a process.

Equimolar amounts of **1a,a′**, dppe, and $NaBPh_4$ were reacted in $CH_2Cl_2/CH_3OH$. After workup in the usual manner, an orange-mustard solid was obtained. The $^{31}P\{^1H\}$ NMR ($CDCl_3$/acetone) spectrum of this solid showed two singlets ($\delta$ 31.6, 31.3) in a 3.7:1 ratio. The potentially chelating ligand, dppe, may coordinate to the Ru(II) center(s) in three possible modes[19] to form a monodentate, monometallic species (**10**), a bidentate monometallic species (**11**), or bidentate bimetallic species (**12** and **13**). Since the ruthenium centers in **10**, **12**, and **13** are chiral, for each structure there will be diastereomers which are distinguishable by $^{31}P$ NMR spectroscopy.[20] These structures and their expected number of $^{31}P$ resonances are shown in Scheme 2.

The only species that would not be expected to exhibit phosphorus-phosphorus coupling and hence give rise to singlets in their $^{31}P\{^1H\}$ NMR spectra are **12**. Hence, the two singlets observed at $\delta$ 31.6 and 31.3 ppm are assigned to the two symmetric diastereomers **12(*R*)** and **12(*S*)** with $R_{Ru(1)},R_{Ru(2)}$ and $S_{Ru(1)},S_{Ru(2)}$ absolute configurations. For the dppe products discussed here, which have an $R_C$ absolute configuration at the benzylic C atom (i.e. arylamino ligand **a**), we assign the structural designations **12(*R*)$_a$(**dppe-$BPh_4$**)** and **12(*S*)$_a$(**dppe-$BPh_4$**)**, respectively. However, at this point the above assignments are tentative, since the origin of each resonance cannot be specified. The diastereoselectivity in this reaction (3:7:1 ratio, 57.4% de) is comparable to that observed for the $Ph_3P$ analog (**5a,a′**, 53.5% de).

Crystallization of this sample from acetone/$CH_3OH$/ether-hexane (1:1) produced a small sample of orange crystals. The $^{31}P\{^1H\}$ NMR ($CDCl_3$/acetone) spectrum of these crystals showed one resonance at $\delta$ 31.6, which corresponds to the major diastereomer. The UV−visible spectrum ($CH_2Cl_2$) of these crystals shows two strong absorption maxima ($\lambda_{max}$, nm ($\epsilon$, L mol$^{-1}$ cm$^{-1}$): 327 (2.9 × 10$^3$), 407 (2.1 × 10$^3$)). The CD spectrum of the same solution shows a weak (broad) negative Cotton effect at 368 nm. This compares with the negative Cotton effect at 368 nm exhibited by the starting **1a,a′** mixture in its CD spectrum. Hence, we assign to the major diastereomer the $S_{Ru(1)},S_{Ru(2)},R_C$ absolute configuration, designated as **12(*S*)$_a$(**dppe-$BPh_4$**)**. This indicates that the above reaction also proceeds with predominant retention of configuration at Ru.

When the reaction of **1a,a′** with dppe was carried out in the presence of $NaBF_4$ in $CH_2Cl_2/CH_3OH$, an orange-mustard solid was obtained after the usual workup. The $^{31}P\{^1H\}$ NMR ($CDCl_3$) spectrum of this solid showed two doublets ($\delta$ 30.84 ($^3J_{PP}$ = 29.0 Hz), −12.37 ($^3J_{PP}$ = 29.0 Hz)), and an AB multiplet ($\delta$ 30.94 ($^3J_{PP}$ = 33.3 Hz), 29.93 ($^3J_{PP}$ = 33.3 Hz)) with relative intensities of 16:1 for the two species. We assign the two doublets at $\delta$ 30.84 and −12.37 ($^3J_{PP}$ = 29.0 Hz) (major species) to the monodentate, monometallic structure **10**. Depending on the absolute configuration at Ru, two diastereomers (**10(*R*)** and **10(*S*)**) are possible. For this compound, with a $R_C$ configuration at the benzylic C atom (i.e. ligand **a**) and with $BF_4$ as the counterion, we designate the two diastereomers as **10(*R*)$_a$**(dppe-$BF_4$) and **10(*S*)$_a$** (dppe-$BF_4$). Since only one set of doublets assignable to **10** is observed, only one of these two diastereomers is present with appreciable concentration; at this point we do not know which one.

The AB pattern ($\delta$ 30.94, 29.93 ($^3J_{PP}$ = 33.3 Hz)) can be assigned only to the asymmetric bidentate, bimetallic species **13(*RS*)**. In this case only one diastereomer is possible, since the designations of the two Ru centers in **13** as Ru(1) and Ru(2) are arbitrary. Thus, the overall designation of the minor species in the above $CDCl_3$ solution is **13(*RS*)$_a$**(dppe-$BF_4$).

When it stood overnight (∼15 h) at ambient temperature, the original orange-mustard color of the above $CDCl_3$ solution turned dark green with concomitant

**Scheme 2**

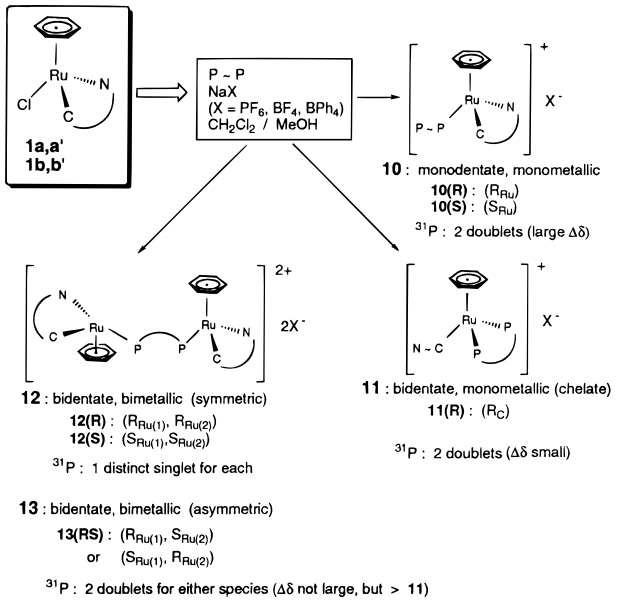


(18) Doxsee, K. M.; Hanawalt, E. M.; Shen, G. S.; Weakly, T. J. R.; Hope, H.; Knobler, C. B. *Inorg. Chem.* **1991**, *30*, 3381.
(19) King, R. B.; Efraty, A. *Inorg. Chem.* **1969**, *8*, 2374.
(20) Nelson, J. H. *Coord. Chem. Rev.* **1995**, *139*, 245.

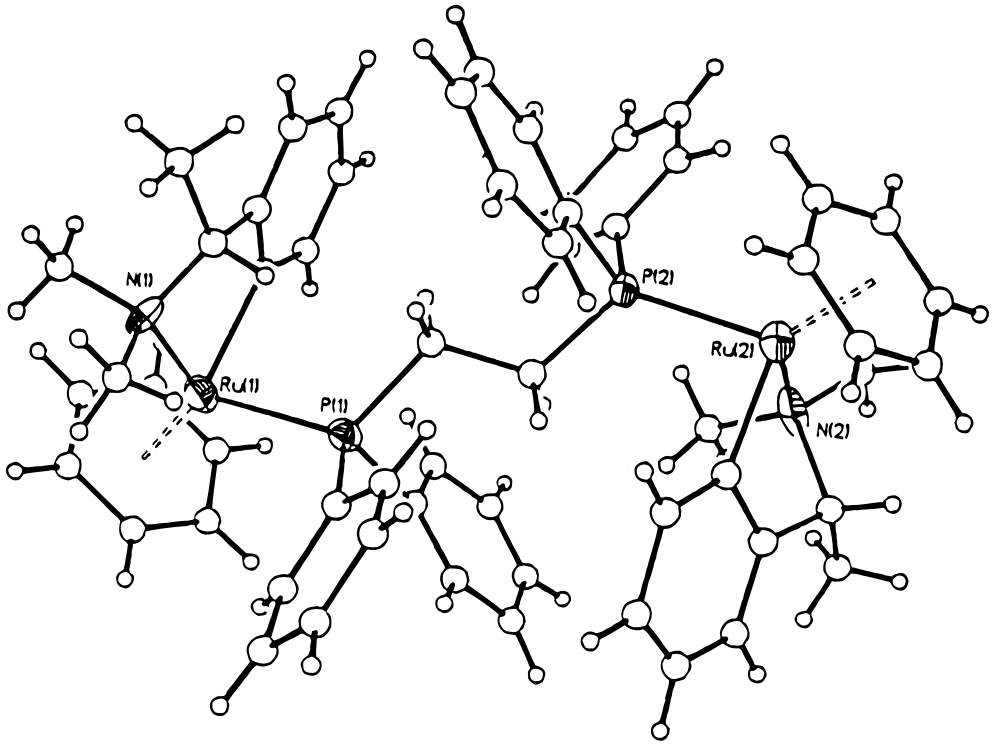


**Figure 8.** Structural drawing of the cation of **13(*RS*)$_a$**(dppe-$BF_4$), showing the atom-numbering scheme (50% probability ellipsoids; hydrogen atoms have arbitrary radii of 0.1 Å). Selected bond lengths (Å) and angles (deg) around Ru(1) and Ru(2), respectively: Ru−C(aryl), 2.07(3), 2.02(3); Ru−C(arene, av) 2.25(2), 2.26(2); Ru−N, 2.17(2), 2.16(2); Ru−P, 2.365(7), 2.346(6); C(aryl)−Ru−N, 78.9(10), 78.1(10); C(aryl)−Ru−P, 83.4(6), 90.6(8); N−Ru−P, 97.0(5), 95.9(5). Configurations: Ru1, $S_{Ru}$; Ru2, $R_{Ru}$.



formation of a small sample of orange-red crystals. An X-ray crystallographic study, performed on a suitable single crystal from this sample, showed the solid-state structure to be **13(*RS*)$_a$**(dppe-$BF_4$) (Figure 8). Thus, the minor species has a lower solubility than the major one. The bond lengths and angles around the two Ru centers differ slightly but compare well with those of the other phosphine-substituted products discussed previously.

The original orange-mustard solid (for which two species are present in $CDCl_3$, as discussed above) shows a UV−visible ($CH_2Cl_2$) spectrum with two strong absorbance maxima ($\lambda_{max}$, nm ($\epsilon$, L mol$^{-1}$ cm$^{-1}$): 327 (2.9 × 10$^3$), 407 (2.1 × 10$^3$)). The CD spectrum of the same $CH_2Cl_2$ solution shows a relatively strong negative Cotton effect at 347 nm. This compares with the strong negative Cotton effect at 368 nm in the CD spectrum of the starting **1a,a′** mixture, for which the major species has an $S_{Ru}$,$R_C$ absolute configuration. Since **13(*RS*)$_a$**-(dppe-$BF_4$) should not exhibit a CD spectrum in this region, we conclude that the major species in solution is **10(*S*)$_a$**(dppe-$BF_4$).

Thus, to conclude this section on the substitution reactions of **1a,a′**, we note the following. (1) The reaction in the presence of $NaBPh_4$ produces a mixture of two bidentate, bimetallic diastereomers and proceeds with predominant retention of configuration at Ru. The stereoselectivity here (57.4% de) is comparable to that in the analogous $Ph_3P$ substitution reaction (53.5% de). (2) The reaction in the presence of $NaBF_4$ produces a 16:1 mixture of a monodentate, monometallic compound (as a single diastereomer) and an asymmetric bidentate, bimetallic complex; the latter crystallizes from $CDCl_3$ solution preferentially. (3) The bidendate, monometallic (chelate) structure **11** (Scheme 2), wherein the Ru−N bond of the arylamino group has been broken, was not detected in any of these reactions.

**3. Substitution of Cl by Nitrogen Donors: Synthesis and Characterization of {(η$^6$-C$_6$H$_6$)Ru[C$_6$H$_4$CH(Me)N(Me)$_2$](L)}$^+$X$^-$ (X$^-$ = PF$_6$, BF$_4$, BPh$_4$). A. L = CH$_3$CN.** Acetonitrile complexes of the type {($\eta^6$-$C_6H_6$)$RuCl(CH_3CN)_2$}$^+X^-$ have been found to be versatile synthetic intermediates in organoruthenium chemistry,[21ab] as one or both of the $CH_3CN$ ligands may be readily replaced by another ligand. Thus, in addition to being products of Cl substitution with an N-donor ligand in our studies, complexes of the type {($\eta^6$-$C_6H_6$)Ru[$C_6H_4CH(Me)N(Me)_2$]($CH_3CN$)}$^+X^-$ could serve as precursors for other ligand substitution products. Reaction of **1a,a′** with $CH_3CN$ in the presence of $KPF_6$, $NaPF_6$, $NaBF_4$, $AgBF_4$, or $NaBPh_4$ in a variety of solvents such as $CH_2Cl_2$, $CH_3OH$, acetone, or $CH_3CN$ all led to dark green solutions. In each case a dark green gummy solid was obtained after the usual workup, which could not be purified by column chromatography or fractional crystallization. This is surprising in light of the facts that $CH_3CN$ complexes of Ru(II) are numerous and {($\eta^6$-$C_6H_6$)Ru[$C_6H_4CH(Me)N(Me)_2$]($CH_3CN$)}$^+PF_6^-$ is stable.[22] It is worth noting that the two diastereomers ($R_{Ru}$,$R_C$)- and ($S_{Ru}$,$R_C$)-[($\eta^5$-$C_5H_5$)RuCl(prophos)] (prophos is a chelating diphosphine ligand

(21) (a) McCormick, F. B.; Cox, D. D.; Gleason, W. B. *Organometallics* **1993**, *12*, 610. (b) Seddon, E. A.; Seddon, K. R. *The Chemistry of Ruthenium*; Elsevier: Amsterdam, 1984; Chapter 9.

(22) Sutter, J. -P. Ph.D. Dissertation, L'Université Louis Pasteur de Strasbourg, Strasbourg, France, 1992.

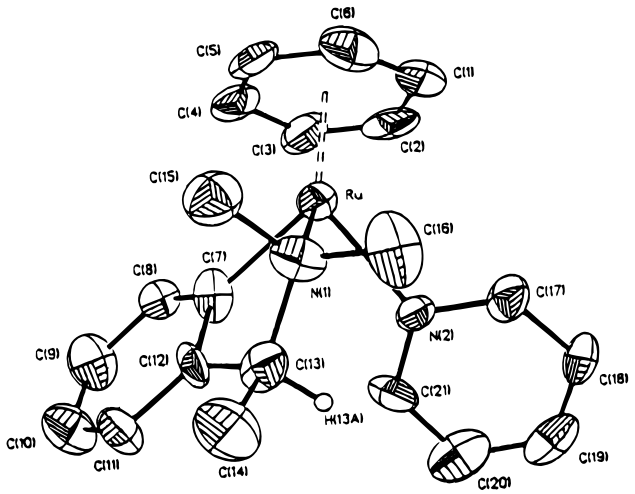


**Figure 9.** Structural drawing of the cation of **14b′**, showing the atom-numbering scheme (50% probability ellipsoids; the benzylic hydrogen atom (H13A) has an arbitrary radius of 0.1 Å). Selected bond lengths (Å) and angles (deg): Ru-C(aryl), 2.040(12); Ru−C(arene, av), 2.227(11); Ru−N1, 2.210(12); Ru−N2, 2.148(9); C(aryl)−Ru−N1, 78.5(5); C(aryl)−Ru−N2, 87.8(5); N1−Ru−N2, 86.0(4).

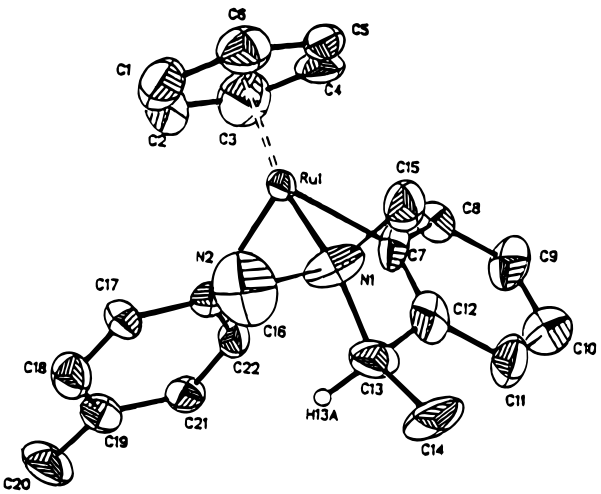


**Figure 10.** Structural drawing of the cation of **15a**, showing the atom-numbering scheme (50% probability ellipsoids; the benzylic hydrogen atom (H13A) has an arbitrary radius of 0.1 Å). Selected bond lengths (Å) and angles (deg): Ru−C(aryl), 2.082(8); Ru−C(arene, av), 2.212-(10); Ru−N1, 2.18(2); Ru−N2, 2.12(2); C(aryl)−Ru−N1, 77.2(7); C(aryl)−Ru−N2, 88.3(6), N1−Ru−N2, 89.5(7).

containing a carbon stereocenter) undergo[23] a $Cl^-$ substitution by $CH_3CN$ in the presence of $NaPF_6$ to yield a mixture of diastereomeric products (>95% de); the reaction proceeds with retention of configuration at Ru.

**B. L = Pyridine.** The reaction of **1b,b′** with pyridine in the presence of $NaBPh_4$ in $CH_2Cl_2/CH_3OH$ yielded, after the usual workup, a greenish orange solid whose $^1H$ NMR ($CDCl_3$) spectrum indicated the presence of two diastereomers[10] in a 1:2.5 ratio (42.9% de). These two diastereomers, ($S_{Ru},S_C$)- and ($R_{Ru},S_C$)-{($\eta^6$-$C_6H_6$)-Ru[$C_6H_4CH(Me)N(Me)_2$](py)}$^+BPh_4^-$, are designated as **14b** and **14b′**, respectively. The original greenish orange color of this $CDCl_3$ solution turned darker green on overnight standing (∼15 h) at ambient temperature. However, the $^1H$ NMR spectrum did not change. Addition of $CH_3OH$ and ether-hexane (1:1) with slow diffusion of the solvents over several days produced well-formed, rod-shaped, orange crystals. The $^1H$ NMR spectrum of this crystalline sample did not differ significantly from that before crystallization. An X-ray crystallographic study, conducted on a suitable single crystal from this sample, showed (Figure 9) the structure to be **14b′** with an $R_{Ru},S_C$ absolute configuration, the same as that of **1b′**.

The metrical parameters are very similar to those of the starting chloro compound **1b′**.[10] The increase in both the Ru−C(arene, av) distance (**1b′**, 2.201(4) Å; **14b′**, 2.227(11) Å) and the Ru−N(1) distance (**1b′**, 2.193(3) Å; **14b′**, 2.201(12) Å), as one goes from **1b′** to **14b′**, probably reflects the increase in steric congestion around the Ru atom. The Ru-N(2) bond length of 2.148(9) Å in **14b′** may be compared to a Ru−N(4-Me-py) distance of 2.142(4) Å recently reported[8e] for the compound [($\eta^6$-1-Me-4-Pr$^i$-$C_6H_4$)Ru(LL*)(4-Me-py)]$^+ClO_4^-$.

The UV−visible spectrum ($CH_2Cl_2$) of the **14b,b′** mixture ($\lambda_{max}$, nm ($\epsilon$, L mol$^{-1}$ cm$^{-1}$): 305 ($7.5 \times 10^3$), 402 ($1.6 \times 10^3$)) resembles those of the phosphine-substituted analogs discussed previously. The CD spectrum of the same $CH_2Cl_2$ solution shows two Cotton effects, a negative one at 430 nm and a positive one at 335 nm. These Cotton effects compare very well in both their signs and shapes with those exhibited by the **1b,b′** mixture in its CD spectrum, a negative one at 462 nm and a positive one at 368 nm. Thus, the absolute configuration of the major diastereomer **14b′** is $R_{Ru},S_C$ and this substitution reaction proceeds with predominant retention of configuration at Ru.

**C. L = 4-Methylpyridine (4-Me-py).** Reactions of equimolar quantities of **1a,a′**, 4-Me-py, and $NaBF_4$ in $CH_2Cl_2/CH_3OH$ yielded, after the usual workup, a dark brown-green foamy product. The $^1H$ NMR ($CDCl_3$) spectrum of this mixture indicated the presence of two diastereomers in a 3.1:1 ratio (51.2% de). These two diastereomers, ($S_{Ru},R_C$)- and ($R_{Ru},R_C$)-{($\eta^6$-$C_6H_6$)Ru[$C_6H_4$-CH(Me)N(Me)$_2$](4-Me-py)}$^+BF_4^-$, are designated as **15a** and **15a′**, respectively. The stereoselectivity in this reaction is higher than that in the pyridine case (42.9% de) and comparable to that for the $BPh_4$ analog of the $Ph_3P$-substituted compound **5a,a′** (53.5% de).

Purification of the initial dark brown-green foamy solid mixture by chromatography (alumina, $CH_2Cl_2/CH_3OH$ (1%)) followed by metathesis with $NaBPh_4$ and fractional crystallization ($CH_2Cl_2/Et_2O$) yielded a sample of well-formed, plate-shaped reddish orange crystals. The $^1H$ NMR ($CDCl_3$) spectrum of this sample indicated the presence of only the major diastereomer in solution. An X-ray crystallographic study, performed on a suitable single crystal from this sample, showed (Figure 10) the structure to be that of the $S_{Ru},R_C$ diastereomer, **15a**. The metrical parameters are very similar to those of **14b′**. The Ru−N(4 Me-py) bond length of 2.12(2) Å in **15a** is slightly shorter than the Ru−N(py) bond length of 2.148(9) Å in **14b′**, which may indicate a slightly stronger Ru−N bond in the 4-Me-py complex.

The UV−visible spectrum ($CH_2Cl_2$) of the **15a,a′** mixture shows the expected two strong absorption

(23) Morandini, F.; Consiglio, G.; Ciani, G.; Sironi, A. *Inorg. Chim. Acta* **1984**, *82*, L27.

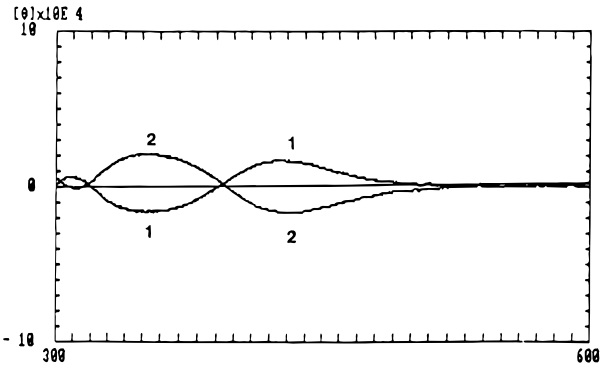


**Figure 11.** . CD spectra of **15a,a′** (51.2% de, curve 1) and **14b,b′** (42.9% de, curve 2) in $CH_2Cl_2$ ($1.1 \times 10^{-4}$ M, 1 cm pathlength cell), showing their enantiomeric relationship.

maxima ($\lambda_{max}$, nm ($\epsilon$, L mol$^{-1}$ cm$^{-1}$): 323 ($4.0 \times 10^3$), 404 ($1.0 \times 10^3$)). The CD spectrum of the same $CH_2Cl_2$ solution shows two Cotton effects, a positive one at 425 nm and a negative one at 347 nm. This compares both in sign and shape with the two Cotton effects in the CD spectrum of the **1a,a′** mixture at 462 nm (positive) and 368 nm (negative), suggesting that the Ru absolute configuration of **15a** (the major diastereomer) is $S_{Ru}$. Hence, this substitution reaction also proceeds with predominant retention of configuration at Ru.

The absolute configurations of **14b′** ($R_{Ru}$,$S_C$) and **15a** ($S_{Ru}$,$R_C$) are enantiomeric. A mirror image relationship is displayed in their CD spectra (Figure 11), despite the fact that they contain different ligands (4-Me-py and py) and different counterions ($BF_4$ and $BPh_4$).

**4. The Stereochemistry of Substitution Reactions and Its Relation to Possible Reaction Mechanisms.** The results of our studies on the stereochemistry of $Cl^-$ substitution reactions of the **1a,a′,b,b′** complexes clearly show that these reactions proceed with predominant retention of configuration at Ru. A search through the literature related to this subject[5,7,8] reveals that retention of configuration at the metal center has been the most common stereochemical outcome in these studies. Epimerization and/or racemization is sometimes observed; however, net inversion of metal configuration appears to be rare.

Racemization of (+)- and (−)-[($\eta^5$-$C_5H_5$)Mn(NO)(COPh)(PPh$_3$)] has been shown to occur *via* a dissociative process,[7b] involving the interconversion of the chiral intermediates **16** and **16'** (equilibrium 1). The inter-

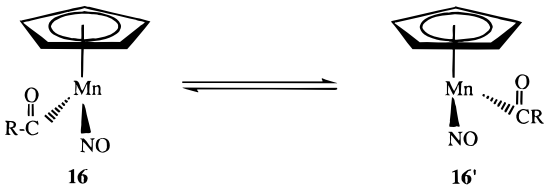


**16** **16'** (1)

conversion of such chiral, pyramidal intermediates (**16**, **16′**) should proceed through a planar species, and [($\eta^5$-$C_5Me_5$)Fe(dppe)]$^+$ has recently been shown to be planar.[24a] In a theoretical study[24b] on the dynamic behavior of unsaturated organometallic intermediates of the type [($\eta^5$-$C_5H_5$)ML$^1$L$^2$] it was concluded that such species may be configurationally stable. The involvement of chiral intermediates of the type **16** and **16′** has also been suggested for the ligand substitution reactions of chiral Ru(II) cyclopentadienyl complexes.[7i] If our ligand substitution reactions were dissociative in nature, one would not expect to observe much of an entering-group effect on the overall rate of the reaction.[25] The stereochemical outcome, however, may be determined after the rate-determining step and may not be related to the overall rate of the reaction. The results of our stereochemical investigations are summarized in Table 1. Two main conclusions may be drawn from these results. First, nearly all of the reactions studied proceed predominantly with retention of configuration at the Ru center. Second, in the three series of ligand substitutions considered (halides, P-donor and N-donor ligands) there seems to be a definite steric effect such that the stereoselectivity (% de) increases with increasing bulk of the incoming ligand. These two conclusions at first sight suggest an associative interchange ($I_a$) mechanism (Scheme 3).

The proposed formation of 7-coordinate, 20-electron activated complexes of the type **17** may be supported by studies[26] on the mechanism of conversion of an alkyne ligand into a vinylidene ligand via 7-coordinate alkynyl−hydrido intermediates of the type [($\eta^5$-$C_5H_5$)Rh(C≡CPh)(R$_3$P)$_2$(H)]. Alternatively, an 18-electron 6-coordinate activated complex of the type **18**, wherein the slippage of the arene ring from the $\eta^6$ to the $\eta^4$ mode of bonding occurs, could be proposed. This postulate may be supported by the many examples of such a ring slippage which have been reported for organometallic complexes containing arene[27] and cyclopentadienyl[28]

**Table 1. Diastereoselectivities[a] and the Stereochemical Course of $Cl^-$ Substitution Reactions of {($\eta^6$-$C_6H_6$)RuCl[$C_6H_4$CH(Me)N(Me)$_2$]} Complexes[b] (1a,a′,b,b′)**

| L | X | diastereoselectivity, % de | reacn stereochem at Ru[c] (% retention for major species) |
|---|---|---|---|
| | | Halides | |
| I | | 94.3 | retention (100) |
| Br | | 93.2 | retention (100) |
| | | P-Donor Ligands | |
| dppe | $BF_4$ | 88.2 | retention (99.0) |
| $Ph_3P$ | $PF_6$ | 60.0 | retention (83.4) |
| dppe | $BPh_4$ | 57.4 | retention (81.9) |
| $Ph_3P$ | $BPh_4$ | 53.5 | retention (80.8) |
| DBP | $PF_6$ | 33.3 | retention (68.4) |
| DBP | $BPh_4$ | 33.3 | retention (68.4) |
| $Et_3P$ | $BPh_4$ | 25.9 | retention (64.4) |
| DMPP | $BPh_4$ | 13.0 | retention (57.2) |
| | | N-Donor Ligands | |
| 4-Me-py | $BF_4$ | 51.2 | retention (78.5) |
| py | $BPh_4$ | 42.9 | retention (73.8) |

[a] Arranged in the order of decreasing % de within each of the three ligand groups studied; % de = (% major diastereomer) − (% minor diastereomer). [b] The % de in the starting **1a,a′** (20:1) or **1b,b′** (1:20) mixtures was 90%. [c] The predominant stereochemical outcome, since some inversion also takes place; for the iodide and bromide reactions, the minor diastereomer undergoes 43% and 32% inversion, respectively.

(24) (a) Hamon, P.; Toupet, L.; Hamon, J.-R.; Lapinte, C. *Organometallics* **1996**, *15*, 10. (b) Hofmann, P. *Angew. Chem., Int. Ed. Engl.* **1977**, *16*, 536.

(25) Katakis, D.; Gordon, G. *Mechanisms of Inorganic Reactions*; Wiley: New York, 1987.

(26) Wolf, J.; Werner, H.; Serhadli, D.; Ziegler, M. L. *Angew. Chem., Int. Ed. Engl.* **1983**, *22*, 414.

(27) Muetterties, E. L.; Bleeke, J. R.; Wucherer, E. J.; Albright, T. A. *Chem. Rev.* **1982**, *82*, 499.

**Scheme 3**

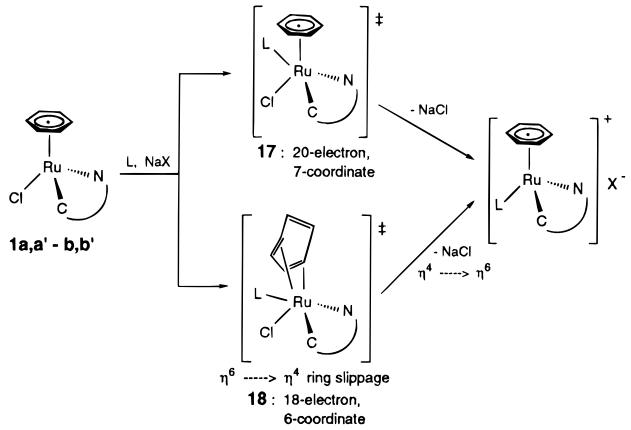


ligands. Subsequent elimination of the $Cl^-$ leaving group, followed by (or concurrent with) the restoration of the arene ring to its $\eta^6$ mode, would generate the diastereomeric products. It should be noted, however, that both activated complexes **17** and **18** would lead to the same stereochemical outcome in these reactions. As a reviewer has pointed out, the experimental results might be more easily rationalized by a dissociative mechanism (Scheme 4). Formation of the minor products (inversion of ruthenium configuration) suggests that pyramidal inversion of the 16-electron intermediates (**19** and **20** with rate constants $k_2$ and $k_{-2}$) could be competitive with ligand recapture of the initially formed pyramidal complex **19**. The incoming ligand effect on the diastereoselectivity could be due to a difference in reactivity of the diastereomeric intermediates **19** and **20** (influenced by the carbon stereocenter) with the initially formed pyramidal intermediate, **19**, being more reactive (less sterically hindered). The difference in reactivity between **19** and **20** and hence the diastereoselectivity should increase with increasing steric bulk of the entering ligand.

The stereochemical results of these reactions should be complimented by kinetic studies in order to gain a greater understanding of the intimate mechanism of these reactions. Such studies are in progress.



## Experimental Section

**1. Physical Measurements.** The $^1H$ and $^{13}C\{^1H\}$ NMR spectra were recorded either on a General Electric QE-300 FT NMR spectrometer (operating at 300 MHz for $^1H$ and 75 MHz for $^{13}C$) or on a Varian Unity Plus-500 FT NMR spectrometer (operating at 500 MHz for $^1H$ and 125 MHz for $^{13}C$). Chemical shifts were referenced to residual solvent resonances. The $^{31}P\{^1H\}$ NMR spectra were recorded on a General Electric GN-300 FT NMR spectrometer at 121 MHz and were referenced to external $Ph_3P(CDCl_3)$, which resonates at −6.00 ppm with respect to an 85% aqueous solution of $H_3PO_4$. FT-IR spectra were recorded on a Perkin-Elmer PE-1800 spectrometer for the far-IR region (below 400 $cm^{-1}$) as mineral oil mulls on a polyethylene sheet (abbreviations: shp = sharp, sh = shoulder, st = strong, w = weak, amb = ambiguous). UV−visible spectra were recorded (at 25 °C) on a Perkin-Elmer Lambda-11 UV−visible spectrophotometer with a $1.1 \times 10^{-4}$ M $CH_2Cl_2$ solution of each compound placed in a cuvette with a cell path length ($b$) of 1.00 cm. CD spectra were recorded (at 25 °C) on a JASCO J-40 spectropolarimeter, with a $1.1 \times 10^{-4}$ M $CH_2Cl_2$ solution of each compound placed in a cell where $b$ = 1.00 cm. Melting points were determined on a Mel-Temp apparatus; all complexes decomposed at temperatures above 180 °C. Elemental analyses were performed by Galbraith Laboratories, Knoxville, TN.

**2. Synthesis and Characterization of the Products of Substitution Reactions {($\eta^6$-$C_6H_6$)Ru[$C_6H_4CH(Me)N(Me)_2$]-(X)] (X = Br, I; 2a,a′, 3a,a′).** These complexes were prepared by the same general route, *i.e.* metathetic reactions of the chloro analog diastereomeric mixture **1a,a′**[10] with NaBr or NaI; no precautions were taken to exclude air from the reaction mixtures. The following procedure for the preparation of **2a,a′** is representative.

**2a,a′ (X = Br).** A sample of **1a,a′** (0.20 g, 0.55 mmol) was dissolved in a mixture of EtOH (95%, 50 mL) and $CH_2Cl_2$ (2 mL) to give a transparent reddish orange solution. To this solution was added 1 mL of a saturated solution of NaBr in $H_2O$ ($d \approx 0.80$ g/mL; 1 mL = 7.8 mmol), and the resulting opaque mixture was stirred at ambient temperature for 1 h, after which the solvents were removed under reduced pressure. The pale orange solid residue was washed with several portions of $CH_2Cl_2$, and each washing was gravity-filtered through Celite to remove the insolubles (NaCl, excess NaBr). Removing $CH_2Cl_2$ from the resulting dark reddish orange filtrate under reduced pressure and drying the residue *in vacuo* gave the pure product as a maroon red powder, yield 0.19 g (84.5%). Anal. Calcd for $C_{16}H_{20}BrNRu$: C, 47.17; H, 4.96; N, 3.44. Found: C, 47.02; H, 4.83; N, 3.51.

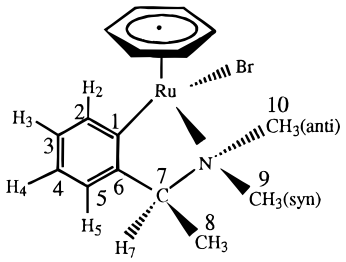


$^1H$ NMR (500 MHz, $CDCl_3$): **2a** (major), $\delta$ 1.19 (d, $^3J(H_7H_8)$ = 7.0 Hz, 3H, $CH_3$(8)), 2.48 (s, 3H, $CH_3$(9)), 3.44 (s, 3H, $CH_3$-(10)), 4.41 (qd, $^3J(H_7H_8)$ = 7.0 Hz, $^6J(H_3H_7)$ = 1.0 Hz, 1H, $H_7$), 5.38 (s, 6H, $\eta^6$-$C_6H_6$), 6.78 (dd, $^3J(H_5H_4)$ = 7.5 Hz, $^4J(H_5H_3)$ = 1.5 Hz, 1H, $H_5$), 6.94 (apparent td, $^3J(H_4H_3) = {}^3J(H_4H_5)$ = 7.5 Hz, $^4J(H_2H_4)$ = 1.5 Hz, 1H, $H_4$), 7.10 (apparent tdd, $^3J(H_3H_2) = {}^3J(H_3H_4)$ = 7.5 Hz, $^4J(H_3H_5)$ = 1.5 Hz, $^6J(H_3H_7)$ = 1.0 Hz, 1H, $H_3$), 8.21 (dd, $^3J(H_2H_3)$ = 7.5 Hz, $^4J(H_2H_4)$ = 1.5 Hz, 1H, $H_2$); **2a′** (minor), $\delta$ 1.28 (d, $^3J(H_7H_8)$ = 7.0 Hz, 3H, $CH_3$(8)), 2.14 (s, 3H, $CH_3$(9)), 3.36 (s, 3H, $CH_3$(10)), 3.84 (q, $^3J(H_7H_8)$ = 7.0 Hz, 1H, $H_7$), 5.30 (s, 6H, $\eta^6$-$C_6H_6$), 6.74 (dd, $^3J(H_5H_4)$ = 7.5 Hz, $^4J(H_5H_3)$ = 1.5 Hz, 1H, $H_5$), 6.93 (apparent td, $^3J(H_4H_3) = {}^3J(H_4H_5)$ = 7.5 Hz, $^4J(H_4H_2)$ = 1.5 Hz, 1H, $H_4$), 7.12 (apparent td, $^3J(H_3H_2) = {}^3J(H_3H_4)$ = 7.5 Hz, $^4J(H_3H_5)$ = 1.5 Hz, 1H, $H_3$), 7.79 (dd, $^3J(H_2H_3)$ = 7.5 Hz, $^4J(H_2H_4)$ = 1.5 Hz, 1H, $H_2$). The relative intensities of the two $H_2$ resonances (28 to 1) establishes[10] the 93.2% de. $^{13}C\{^1H\}$ NMR (125 MHz, $CDCl_3$) **2a:** (major), $\delta$ 9.3 ($C_8$), 49.5 ($C_9$), 53.3 ($C_{10}$), 68.2($C_7$), 85.8 ($\eta^6$-$C_6H_6$), 123.0 ($C_5$), 123.3 ($C_4$), 125.9 ($C_3$), 137.6 ($C_2$), 149.5 ($C_6$), 165.8 ($C_1$). IR (Nujol): $\nu_{Ru-Br}$ 174 $cm^{-1}$ (shp, W). UV−vis: $\lambda_{max}$, nm ($\epsilon$, L $mol^{-1}$, $cm^{-1}$) 380 ($1.7 \times 10^3$), 448 ($1.4 \times 10^3$). CD: $\lambda_{max}$, nm ($[\theta]_\lambda$, deg $cm^2$ $dmol^{-1}$) 600 (0), 466 (+9600), 423 (0), 373 (−19 800).

**3a,a′ (X = I):** yield 0.22 g (88.2%). Anal. Calcd for $C_{16}H_{20}INRu$: C, 42.29; H, 4.45; N, 3.08. Found: C, 42.41; H, 4.36; N, 2.97. $^1H$ NMR (500 MHz, $CDCl_3$): **3a** (major), $\delta$ 1.20 (d, $^3J(H_7H_8)$ = 7.0 Hz, 3H, $CH_3$(8)), 2.46 (s, 3H, $CH_3$(9)), 3.48 (s, 3H, $CH_3$(10)), 4.41 (q, $^3J(H_7H_8)$ = 7.0 Hz, 1H, $H_7$), 5.43 (s, 6H, $\eta^6$-$C_6H_6$), 6.79 (dd, $^3J(H_5H_4)$ = 7.5 Hz, $^4J(H_5H_3)$ = 1.0 Hz, 1H, $H_5$), 6.90 (apparent t, $^3J(H_4H_3) = {}^3J(H_4H_5)$ = 7.5 Hz, 1H, $H_4$), 7.08 (apparent td, $^3J(H_3H_2) = {}^3J(H_3H_4)$ = 7.5 Hz, $^4J(H_3H_5)$ = 1.0 Hz, 1H, $H_3$), 8.12 (dd, $^3J(H_2H_3)$ = 7.5 Hz, $^4J(H_2H_4)$ = 1.5

(28) O'Connor, J. M.; Casey, C. P. *Chem. Rev.* **1987**, *87*, 307.

**Scheme 4**

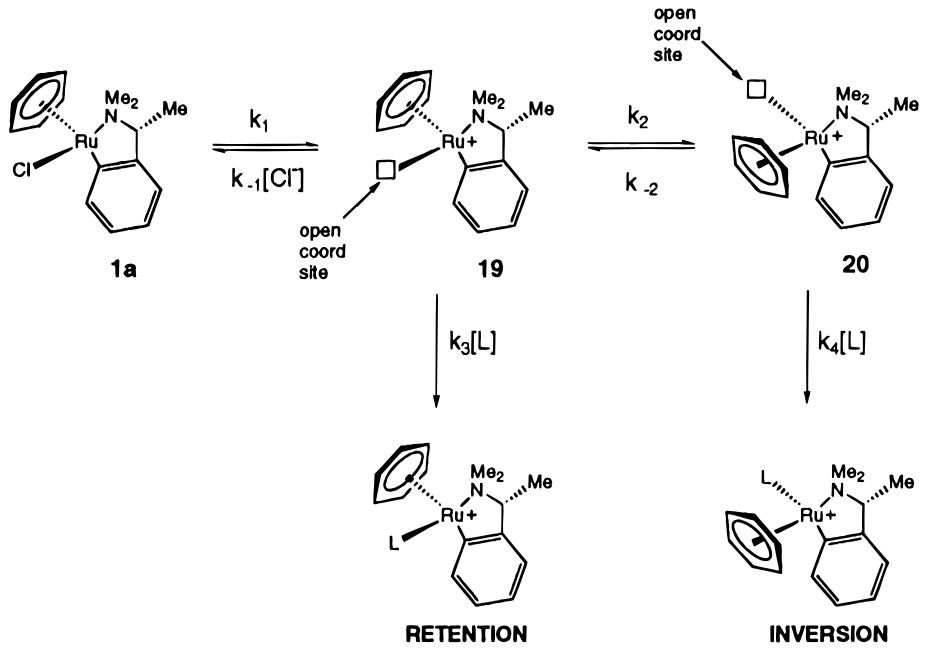




Hz, 1H, $H_2$); **3a′** (minor), $\delta$ 1.26 (d, $^3J(H_7H_8)$ = 7.0 Hz, 3H, $CH_3(8)$), 2.40 (s, 3H, $CH_3(9)$), 3.30 (s, 3H, $CH_3(10)$), 3.88 (q, $^3J(H_7H_8)$ = 7.0 Hz, 1H, $H_7$), 5.30 (s, 6H, $\eta^6$-$C_6H_6$), 6.74 (dd, $^3J(H_5H_4)$ = 7.5 Hz, $^4J(H_5H_3)$ = 1.0 Hz, 1H, $H_5$), 6.89 (apparent td, $^3J(H_4H_3)$ = $^3J(H_4H_5)$ = 7.5 Hz, 1H, $H_4$), 7.07 (apparent td, $^3J(H_3H_2)$ = $^3J(H_3H_4)$ = 7.5 Hz, $^4J(H_3H_5)$ = 1.0 Hz, 1H, $H_3$), 7.87 (dd, $^3J(H_2H_3)$ = 7.5 Hz, $^4J(H_2H_4)$ = 1.5 Hz, 1H, $H_2$). The relative intensities of the two $H_2$ resonances (34:1) establishes[10] the 94.3% de. $^{13}C\{^1H\}$ NMR (125 MHz, $CDCl_3$): **3a** (major), $\delta$ 9.5 ($C_8$), 49.1 ($C_9$), 55.3 ($C_{10}$), 70.3 ($C_4$), 86.1 ($\eta^6$-$C_6H_6$), 122.9 ($C_5$), 123.4 ($C_4$), 126.1 ($C_3$), 138.5 ($C_2$), 149.3 ($C_6$), 164.2 ($C_1$). IR (Nujol): $\nu_{Ru-I}$ 163 $cm^{-1}$ (shp, W, $\lambda$ amb). UV−vis: $\lambda_{max}$, nm ($\epsilon$, L $mol^{-1}$, $cm^{-1}$) 382 ($1.2 \times 10^3$), 472 ($1.0 \times 10^3$). CD: $\lambda_{max}$, nm ($[\theta]_\lambda$, deg $cm^2$ $dmol^{-1}$) 600 (0), 468 (+5400), 435 (0), 383 (−13 200).

**4**−**15.** The phosphine- and pyridine-substituted cationic complexes $\{(\eta^6\text{-}C_6H_6)Ru[C_6H_4CH(Me)N(Me)_2](L)\}^+X^-$ were all prepared by the same general route. This involved reaction of the **1a,a′** or **1b,b′** mixture with the appropriate ligand in the presence of $NaPF_6$, $NaBF_4$, or $NaBPh_4$ in a mixture of $CH_2Cl_2$ and $CH_3OH$. DBP,[29] $Ph_3P$, and dppe were recrystallized from hot EtOH (95%) under nitrogen before use. All other ligands were reagent grade and were used as received. All reactions were carried out under a dry nitrogen atmosphere. The following procedure is representative.

**4b,b′ (L = $Ph_3P$, $X^-$ = $PF_6$).** A mixture of the chloro compound **1b,b′** (0.20 g, 0.55 mmol) and $Ph_3P$ (0.29 g, 1.1 mmol) in $CH_3OH$ (50 mL) and $CH_2Cl_2$ (5 mL) was stirred at ambient temperature to give a transparent, reddish orange solution within a few minutes. To this solution was added solid $NaPF_6$ (0.18 g, 1.1 mmol), and the resulting opaque mixture was stirred at ambient temperature overnight (∼15 h). The solvents were removed under reduced pressure, and the residue was washed with 30 mL of a 1:1 ether/hexane mixture. The remaining orange-yellow solid was washed with several portions of $CH_2Cl_2$, and the combined washings were filtered through Celite to remove NaCl and excess $NaPF_6$. Removing $CH_2Cl_2$ under reduced pressure, followed by drying the residue *in vacuo*, afforded the product as an orange-yellow powder; yield 0.26 g (63.7%). Anal. Calcd for $C_{34}H_{35}F_6NP_2Ru$: C, 55.58; H, 4.81; N, 1.91. Found: C, 55.43; H, 4.69; N, 1.78. $^{31}P\{^1H\}$ NMR (121 MHz, $CDCl_3$): $\delta$ 32.9 (s, **4b**, 1), 31.2 (s, **4b′**, 4), −145.0 (septet, $^1J(PF)$ = 710 Hz, 5, $PF_6^-$), 60% de. $^1H$ NMR (500 MHz, $CDCl_3$): **4b′** (major), $\delta$ 0.74 (d, $^3J(H_8H_7)$ = 7.0 Hz, 3H, $CH_3(8)$), 2.39 (q, $^3J(H_7H_8)$ = 7.0 Hz, 1H, $H_7$), 2.46 (s, 3H, $CH_3(9)$), 3.07 (s, 3H, $CH_3(10)$), 5.59 (d, $^2J(PH)$ = 0.5 Hz, 6H, $\eta^6$-$C_6H_6$), 6.44 (d, $^3J(H_5H_4)$ = 7.5 Hz, 1H, $H_5$), 7.05 (apparent td, $^3J(H_4H_3)$ = $^3J(H_4H_5)$ = 7.5 Hz, $^4J(H_4H_2)$ = 1.2 Hz,1H, $H_4$), 7.24 (apparent t, $^3J(H_3H_2)$ = $^3J(H_3H_4)$ = 7.5 Hz, 1H, $H_3$), 7.3 - 7.5 (m, 15H, $P(C_6H_5)_3$), 7.96 (apparent dt, $^3J(H_2H_3)$ = 7.5 Hz, $^4J(PH)$ = $^4J(H_2H_4)$ = 1.2 Hz, 1H, $H_2$). $^{13}C\{^1H\}$ NMR (125 MHz, $CDCl_3$): **4b′** (major), $\delta$ 9.3 ($C_8$), 52.3 ($C_9$), 57.0 (d, $^3J(PC)$ = 3.5 Hz, $C_7$), 70.9 ($C_{10}$), 93.8 (d, $^2J(PC)$ = 2.6 Hz, $\eta^6$-$C_6H_6$), 124.1 ($C_5$), 125.4 (d, $^5J(PC)$ = 1.8 Hz, $C_4$), 126.5 ($C_3$), 128.4 (d, $^3J(PC)$ = 9.4 Hz, $C_m$), 130.9 ($C_p$), 133.2 (d, $^1J(PC)$ = 50 Hz, $C_i$), 134.1 (d, $^2J(PC)$ = 8.2 Hz, $C_o$), 140.7 ($C_2$), 150.4 (d, $^3J(PC)$ = 2 Hz, $C_6$), 158.3 (d, $^2J(PC)$ = 22.4 Hz, $C_1$). UV−vis: $\lambda_{max}$, nm ($\epsilon$, L $mol^{-1}$, $cm^{-1}$): 326 ($2.7 \times 10^3$), 400 ($1.7 \times 10^3$). CD: $\lambda_{max}$, nm ($[\theta]_\lambda$, deg $cm^2$ $dmol^{-1}$) 600 (0), 356 (+20 400).

**5a,a′ (L = $Ph_3P$, $X^-$ = $BPh_4$):** yield 0.38 g (76%). Anal. Calcd for $C_{58}H_{55}BNPRu$: C, 76.63; H, 6.11; N, 1.54. Found: C, 76.66; H, 6.02; N, 1.51. $^{31}P\{^1H\}$ NMR (121 MHz, $CDCl_3$), $\delta$ 32.8 (s, **5a′**, 1), 31.4 (s, **5a**, 3.3), 53.5% de. $^1H$ NMR (500 MHz, $CDCl_3$): **5a** (major), $\delta$ 0.64 (d, $^3J(H_8H_7)$ = 6.3 Hz, 3H, $CH_3(8)$), 1.97 (s, 3H, $CH_3(9)$), 2.23 (q, $^3J(H_7H_8)$ = 6.3 Hz, 1H, $H_7$), 2.63 (s, 3H, $CH_3(10)$), 5.50 (s, 6H, $\eta^6$-$C_6H_6$), 6.37 (d, $^3J(H_5H_4)$ = 7.5 Hz, 1H, $H_5$), 7.2−7.5 (m, 37H, $P(C_6H_5)_3$, $B(C_6H_5)_4^-$, $H_4$, $H_3$), 7.80 (d, $^3J(H_2H_3)$ = 7.5 Hz, $H_2$). $^{13}C\{^1H\}$ NMR (125 MHz, $CDCl_3$): **5a** (major) $\delta$ 9.3 ($C_8$), 52.4 ($C_9$), 57.0 (d, $^3J(PC)$ = 3.7 Hz, $C_7$), 70.9 ($C_{10}$), 93.4 (d, $^2J(PC)$ = 2.5 Hz, $\eta^6$-$C_6H_6$), 124.2 ($C_5$), 125.3 (d, $^5J(PC)$ = 2.4 Hz, $C_4$), 125.6 ($^3J(BC)$ = 2.5 Hz, $C_m$ ($BPh_4$)), 126.6 ($C_3$), 127.9 ($C_p$ ($BPh_4$)), 128.3 (d, $^3J(CP)$ = 9.8 Hz, $C_m$ ($Ph_3P$)), 130.9 (d, $^4J(PC)$ = 2.5 Hz, $C_p$($PPh_3$)), 131.81 ($^2J(BC)$ = 3.7 Hz, $C_o$ ($BPh_4$)), 133.3 (d, $^1J(PC)$ = 42.7 Hz, $C_i$ ($PPh_3$)), 133.9 (d, $^2J(PC)$ = 9.7 Hz, $C_o$ ($PPh_3$)), 140.9 ($C_2$), 150.4 (d, $^3J(PC)$ = 2 Hz, $C_6$) 157.8 (d, $^2J(PC)$ = 22.0 Hz, $C_1$), 164.2 ($^1J(BC)$ = 48.8 Hz, $C_i$ ($BPh_4$)). UV−vis: identical with that of **4b′**. CD: $\lambda_{max}$, nm ($[\theta]_\lambda$,deg $cm^2$, $dmol^{-1}$) 600 (0), 356 (−14 400).

**6a,a′ (L = DBP, $X^-$ = $PF_6$):** yield 0.29 g (72.5%). Anal. Calcd for $C_{34}H_{33}F_6NP_2Ru$: C, 55.73; H, 4.55; N, 1.91. Found: C, 55.64;, H, 4.48; N, 1.80. $^{31}P\{^1H\}$ NMR (121 MHz, $CDCl_3$): $\delta$ 29.4 (s, **6a**, 2), 28.6 (s, **6a′**, 1), −145.0 (septet, $^1J(PF)$ = 710 Hz, 3, $PF_6^-$), 33.3% de. $^1H$ NMR (500 MHz, $CDCl_3$): **6a** (major), $\delta$ 0.77 (d, $^3J(H_8H_7)$ = 7.0 Hz, 3H, $CH_3(8)$), 2.42 (s, 3H, $CH_3(9)$), 2.95 (s, 3H, $CH_3(10)$), 3.93 (q, $^3J(H_7H_8)$ = 7.0 Hz, 1H,

(29) Affandi, S.; Green, R. L.; Hsieh, B. T.; Holt, M. S.; Nelson, J. H.; Alyea, E. C. *Synth. React. Inorg. Met.-Org. Chem.* **1987**, *17*, 307.

**Table 2. Physical Characteristics of the Crystals of Compounds 3a−15a**

| compd | color | habit | size (mm) | solvent(s) used for crystallizn[a] |
|---|---|---|---|---|
| **3a** | maroon-red | rod | 0.06 × 0.06 × 0.38 | a |
| **4b′** | orange-red | prism | 0.20 × 0.18 × 0.34 | a,b |
| **5a** | yellow | prism | 0.25 × 0.10 × 0.30 | d,b |
| **6a,a′** | orange | wedge | 0.28 × 0.18 × 0.16 | a,c,b |
| **6a** | yellow | prism | 0.28 × 0.18 × 0.16 | c,d |
| **13(*RS*)$_a$**[b] | yellow | plate | 0.38 × 0.24 × 0.18 | d |
| **14b′** | orange | prism | 0.40 × 0.06 × 0.04 | d,c,b |
| **15a** | orange | block | 0.04 × 0.04 × 0.18 | a,e |

[a] Key to solvents used for crystallization: (a) $CH_2Cl_2$; (b) $Et_2O$−hexane (1:1); (c) $CH_3OH$; (d) $CDCl_3$; (e) $Et_2O$. The letters are in order of the addition of solvents. [b] This is **13**(*RS*)$_a$(diphos-$BF_4$).

$H_7$), 5.68 (s, 6H, $\eta^6$-$C_6H_6$), 6.66−8.4 (m, 16H, $C_6H_4$, DBP), 8.07 (d, $^3J(H_2H_3)$ = 7.5 Hz, 1H, $H_2$). UV−vis: $\lambda_{max}$, nm ($\epsilon$, L mol$^{-1}$ cm$^{-1}$): 318 (4.5 × 10$^3$), 403 (1.7 × 10$^3$). CD: $\lambda_{max}$, nm ($[\theta]_\lambda$, deg cm$^2$ dmol$^{-1}$) 600 (0), 370 (−11 400), 337 (−13 200).

**7b,b′ (L = DBP, X$^-$ = BPh$_4$).** The reaction was carried out in a $CH_2Cl_2$/acetone mixture: yield 0.27 g (54.3%). Anal. Calcd for $C_{58}H_{53}BNPRu$: C, 76.80; H, 5.90; N, 1.54. Found: C, 76.59, H, 5.81; N, 1.45. $^{31}P\{^1H\}$ NMR (121 MHz, $CDCl_3$): $\delta$ 29.4 (s, **7b′,** 2), 29.2 (s, **7b**, 1), 33.3% de. $^1H$ NMR (500 MHz, $CDCl_3$): **7b′** (major), $\delta$ 0.67 (d, $^3J(H_8H_7)$ = 7.0 Hz, 3H, $CH_3$-(8)), 1.53 (s, 3H, $CH_3$(9)), 1.99 (s, 3H, $CH_3$(10)), 3.52 (q, $^3J(H_7H_8)$ = 7.0 Hz, 1H, $H_7$), 5.05 (d, $^2J(PH)$ = 0.5 Hz, 6H, $\eta^6$-$C_6H_6$), 6.6−8.0 (m, 37H, $C_6H_4$, DBP, $Ph_4B$). $^{13}C\{^1H\}$ NMR (125 MHz, $CDCl_3$): **7b′** (major), $\delta$ 1.0 ($C_8$), 51.8 ($C_9$), 57.4 (d, $^3J$(PC) = 3.3 Hz, $C_7$), 72.9 ($C_{10}$), 93.0 (d, $^2J$(PC) = 2.4 Hz, $\eta^6$-$C_6H_6$), 121.1−158.3 (complex pattern, $BPh_4$, DBP, $C_6H_4$), 164.1 ($^1J$(BC) = 49.3 Hz, $C_i$ ($BPh_4$)). UV−vis: identical with that of **6a**. CD: $\lambda_{max}$, nm ($[\theta]_\lambda$, deg cm$^2$ dmol$^{-1}$) 600 (0), 370 (+13 200), 337 (−20 400).

**8a,a′ (L = DMPP, X$^-$ = BPh$_4$).** A pure compound could not be obtained. $^{31}P\{^1H\}$ NMR (121 MHz, $CDCl_3$) for the crude product: $\delta$ 42.6 (s, **8a**, 1.3), 41.1 (s, **8a′**, 1), 13.0% de. UV−vis for the crude product: $\lambda_{max}$, nm ($\epsilon$, L mol$^{-1}$ cm$^{-1}$) 325 (3.2 × 10$^3$), 406 (1.1 × 10$^3$). CD for the crude product: $\lambda_{max}$, nm ($[\theta]_\lambda$, deg cm$^2$ dmol$^{-1}$) 600 (0), 382 (−12 000), 318 (+3600).

**9b,b′ (L = Et$_3$P, X$^-$ = BPh$_4$).** A pure compound could not be obtained. $^{31}P\{^1H\}$ NMR (121 MHz, $CDCl_3$) for the crude product: $\delta$ 19.4 (s, **9b**, 1), 17.2 (s, **9b′**, 1.7), 25.9% de. UV−vis for the crude product: $\lambda_{max}$, nm ($\epsilon$, L mol$^{-1}$ cm$^{-1}$) 328 (2.7 × 10$^3$), 408 (1.9 × 10$^3$). CD for the crude product: $\lambda_{max}$, nm ($[\theta]_\lambda$, deg cm$^2$ dmol$^{-1}$) 600 (0), 430 (−7200), 366 (+20 000).

**1a,a′ + dppe + NaBPh$_4$.** A pure compound could not be obtained. $^{31}P\{^1H\}$ NMR (121 MHz, $CDCl_3$) for the crude product: $\delta$ 31.6 **(s, 12(*S*)$_a$(**dppe-$BPh_4$**)**, 3.7), 31.3 (s, **12(*R*)$_a$-(**dppe-$BPh_4$**)**, 1), 57.4% de. UV−vis for the crude product: $\lambda_{max}$, nm ($\epsilon$, L mol$^{-1}$ cm$^{-1}$): 327 (2.9 × 10$^3$), 407 (2.1 × 10$^3$). CD: for the crude product, $\lambda_{max}$, nm ($[\theta]_\lambda$, deg cm$^2$ dmol$^{-1}$) 600 (0), 338 (−20 000).

**1a,a′ + dppe + NaBF$_4$.** The sample size for the pure crystalline product (which crystallized spontaneously from a $CDCl_3$ solution) was too small for elemental analyses to be performed. $^{31}P\{^1H\}$ NMR (121 MHz, $CDCl_3$) for the crude product: $\delta$ 30.84 (d, $^3J$(PP) = 29.0 Hz, 16) and −12.37 (d, $^3J$(PP = 29.0 Hz, 16), both assigned to **10(*S*)$_a$**(dppe-$BF_4$); 30.94 (1) and 29.93 (1) (AB, $^3J$(PP) = 33.3 Hz), both assigned to **13-(*RS*)$_a$**(dppe-$BF_4$). Ratio **10(*S*)$_a$:13(*RS*)$_a$** = 16:1. UV−vis for the crude product: $\lambda_{max}$, nm ($\epsilon$, L mol$^{-1}$ cm$^{-1}$) 377 (2.9 × 10$^3$), 407 (2.1 × 10$^3$). CD for the crude product: $\lambda_{max}$, nm ($[\theta]_\lambda$, deg cm$^2$ dmol$^{-1}$) 600 (0), 347 (−40 000).

**14b,b′ (L = py, X$^-$ = BPh$_4$):** yield 0.23 g (58.1%). Anal. Calcd for $C_{45}H_{45}BN_2Ru$: C, 74.46; H, 6.26; N, 3.86. Found: C, 74.51; H, 6.32; N, 3.75. $^1H$ NMR (500 MHz, $CD_3CN$): **14b′** (major), $\delta$ 1.20 (d, $^3J(H_8H_7)$ = 6.5 Hz, 3H, $CH_3$(8)), 2.44 (s, 3H, $CH_3$(9)), 3.13 (s, 3H, $CH_3$(10)), 3.67 (q, $^3J(H_7H_8)$ = 6.5 Hz, 1H, $H_7$), 5.61 (s, 6H, $\eta^6$-$C_6H_6$), 6.8−8.5 (m, 29H, $C_6H_4$, py, $BPh_4$), 8.12 (dd, $^3J(H_2H_3)$ = 7.5 Hz, $^4J(H_2H_4)$ = 1.5 Hz, 1H, $H_2$); **14b** (minor), $\delta$ 1.24 (d, $^3J(H_8H_7)$ = 6.5 Hz, 3H, $CH_3$(8)), 2.47 (s, 3H, $CH_3$(9)), 3.13 (s, 3H, $CH_3$(10)), 3.90 (q, $^3J(H_7H_8)$ = 6.5 Hz, 1H, $H_7$), 5.53 (s, 6H, $\eta^6$-$C_6H_6$), 6.8−8.5 (m, 29H, $C_6H_4$, py, $BPh_4$), 7.64 (dd, $^3J(H_2H_3)$ = 7.5 Hz, $^4J(H_2H_4)$ = 1.5 Hz, 1H, $H_2$). The relative intensities of the two $H_2$ resonances (2.5:1) establish[10] the 42.9% de. $^{13}C\{^1H\}$ NMR (125 MHz, $CD_3CN$): **14b′** (major), $\delta$ 10.8 ($C_8$), 50.9 ($C_9$), 54.4 ($C_{10}$), 71.3 ($C_7$), 89.5 ($\eta^6$-$C_6H_6$), 122.7−151.0 (complex, $C_6H_4$, py, $BPh_4$), 164.81 ($^1J$(BC) = 49.4 Hz, $C_i$ ($BPh_4$)); **14b** (minor), $\delta$ 10.2 ($C_8$), 51.3 ($C_9$), 56.6 ($C_{10}$), 70.5 ($C_7$), 88.9 ($\eta^6$-$C_6H_6$), 122.7−151.0 (complex, $C_6H_4$, py, $BPh_4$). UV−vis: $\lambda_{max}$, nm ($\epsilon$, L mol$^{-1}$ cm$^{-1}$) 305 (7.5 × 10$^3$), 402 (1.6 × 10$^3$). CD: $\lambda_{max}$, nm ($[\theta]_\lambda$, deg cm$^2$ dmol$^{-1}$) 600 (0), 430 (−8400), 395 (0), 335 (+10 800).

**15a,a′ (L = 4-Me-py, X$^-$ = BF$_4$):** yield 0.18 g (63.0%). Anal. Calcd for $C_{22}H_{27}BF_4N_2Ru$: C, 52.07; H, 5.37; N, 2.76. Found:

**Table 3. Crystallographic Data for 3a−15a**

| | **3a** | **4b′** | **5a** |
|---|---|---|---|
| emp formula | $C_{16}H_{20}INRu$ | $C_{69}H_{70}Cl_2F_{12}N_2P_4Ru_2$ | $C_{58}H_{55}BNPRu$ |
| fw | 454.30 | 1552.19 | 908.88 |
| cryst syst | orthorhombic | monoclinic | orthorhombic |
| *a* (Å) | 7.1203(6) | 9.552(1) | 9.9223(12) |
| *b* (Å) | 14.6366(13) | 34.055(5) | 15.924(3) |
| *c* (Å) | 15.174(2) | 10.952(1) | 29.712(4) |
| α (deg) | 90 | 90 | 90 |
| *β* (deg) | 90 | 90.54(1) | 90 |
| *γ* (deg) | 90 | 90 | 90 |
| *V* (Å$^3$) | 1581.4(3) | 3562.5(7) | 4694.8(12) |
| Z | 4 | 2 | 4 |
| space group | $P2_12_12_1$ | $P2_1$ | $P2_12_12_1$ |
| $\rho_{calcd}$ (Mg/m$^3$) | 1.908 | 1.447 | 1.286 |
| $\mu$ (mm$^{-1}$) | 2.931 | 0.661 | 0.407 |
| transmission max/min | 0.919/0.874 | 0.689/0.623 | 0.781/0.729 |
| $R(F)^{a,b}$ | 0.0582 | 0.0507 | 0.0713 |
| $R_w(F)^{a,b}$ | 0.0750 | 0.1442 | 0.0878 |

| | **6a,a′** | **6a** |
|---|---|---|
| emp formula | $C_{68}H_{66}F_{12}N_2O_{1.75}P_4Ru_2$ | $C_{34}H_{33}F_6NP_2Ru$ |
| fw | 1493.25 | 732.62 |
| cryst syst | triclinic | monoclinic |
| *a* (Å) | 9.979(2) | 10.137(2) |
| *b* (Å) | 10.109(2) | 12.935(3) |
| *c* (Å) | 18.104(2) | 11.871(2) |
| α (deg) | 99.112(10) | 90 |
| *β* (deg) | 102.296(9) | 92.78(3) |
| *γ* (deg) | 95.477(12) | 90 |
| *V* (Å$^3$) | 1746.2(4) | 1554.7(5) |
| Z | 1 | 2 |
| space group | $P1$ | $P2_1$ |
| $\rho_{calcd}$ (Mg/m$^3$) | 1.420 | 1.565 |
| $\mu$ (mm$^{-1}$) | 0.599 | 0.669 |
| transmission max/min | 0.700/0.680 | 0.873/0.838 |
| $R(F)^{a,b}$ | 0.0762 | 0.0896 |
| $R_w(F)^{a,b}$ | 0.2020 | 0.1106 |

| | **13(*RS*)$_a$**(diphos-$BF_4$) | **14b′** | **15a** |
|---|---|---|---|
| emp formula | $C_{60}H_{64}Cl_6F_8N_2P_2Ru_2$ | $C_{45}H_{45}BN_2Ru$ | $C_{92}H_{94}B_2N_4Ru_2$ |
| fw | 1463.53 | 725.71 | 1479.47 |
| cryst syst | monoclinic | orthorhombic | triclinic |
| *a* (Å) | 13.181(3) | 10.295(2) | 9.296(4) |
| *b* (Å) | 18.839(4) | 16.009(2) | 11.253(2) |
| *c* (Å) | 13.181(3) | 22.469(3) | 18.368(3) |
| α (deg) | 90 | 90 | 86.011(4) |
| *β* (deg) | 107.58(2) | 90 | 88.07(2) |
| *γ* (deg) | 90 | 90 | 89.54(2) |
| *V* (Å$^3$) | 3120.3(12) | 3703.0(9) | 1915.7(9) |
| Z | 2 | 4 | 1 |
| space group | $P2_1$ | $P2_12_12_1$ | $P1$ |
| $\rho_{calcd}$ (Mg/m$^3$) | 1.558 | 1.302 | 1.282 |
| $\mu$ (mm$^{-1}$) | 0.856 | 0.457 | 0.443 |
| transmission max/min | 0.787/0.852 | 0.860/0.840 | 0.685/0.550 |
| $R(F)^{a,b}$ | 0.0851 | 0.0752 | 0.0794 |
| $R_w(F)^{a,b}$ | 0.1456 | 0.0853 | 0.1351 |

[a] The data were refined by the method of full-matrix least squares on $F^2$, with the final $R$ indices having $I > 2\sigma(I)$. [b] $R(F) = \Sigma(||F_o| - |F_c||)^2/\Sigma(|F_o|)$; $R_w(F) = [\Sigma w(|F_o| - |F_c|)^2/\Sigma w|F_c|^2]^{1/2}$; $w = 1/\sigma^2(F)^2 = \sigma^2(\text{counts}) + (pI)^2$.

C, 51.98; H, 5.42; N, 2.67. $^1$H NMR (300 MHz, $CDCl_3$): **15a** (major), $\delta$ 1.10 (d, $^3J(H_8H_7) = 7.0$ Hz, 3H, $CH_3$(8)), 2.33 (s, 3H, $CH_3$ (4-Me-py)), 2.57 (s, 3H, $CH_3$(9)), 3.26 (s, 3H, $CH_3$(10)), 3.61 (q, $^3J(H_7H_8) = 7.0$ Hz, $H_7$), 5.59 (s, 6H, $\eta^6$-$C_6H_6$), 6.8−7.6 (m, 8H, $C_6H_4$, 4-Me-py), 8.30 (d, $^3J(H_2H_3) = 7.3$ Hz, 1H, $H_2$); **15a′** (minor), $\delta$ 1.22 (d, $^3J(H_8H_7) = 7.0$ Hz, 3H, $CH_3$(8)), 2.31 (s, 3H, $CH_3$ (4-Me-py)), 2.48 (s, 3H, $CH_3$(9)), 2.92 (s, 3H, $CH_3$(10)), 3.40 (q, $^3J(H_7H_8) = 7.0$ Hz, 1H, $H_7$), 5.57 (s, 6H, $\eta^6$-$C_6H_6$), 6.8−7.6 (m, 8H, $C_6H_4$, 4-Me-py), 7.85 (d, $^3J(H_2H_3) = 7.3$ Hz, 1H, $H_2$). The relative intensities of the two $H_2$ resonances (3.1:1) establishes[10] the 51.2% de. $^{13}$C{$^1$H} NMR (75 MHz, $CDCl_3$): **15a** (major), $\delta$ 10.0 ($C_8$), 20.8 ($CH_3$, 4-Me-py), 50.8 ($C_9$), 52.6 ($C_{10}$), 69.8 ($C_7$), 88.2 ($\eta^6$-$C_6H_6$), 124.6 ($C_5$), 124.7 ($C_4$), 126.9 ($C_3$), 127.6 (4-Me-py, $C_{3,5}$), 137.7 ($C_2$), 149.1 (4-Me-py, $C_4$), 150.6 ($C_6$), 153.9 (4-Me-py, $C_{2,6}$), 168.2 ($C_1$). UV−vis: $\lambda_{max}$, nm ($\epsilon$, L mol$^{-1}$ cm$^{-1}$) 323 ($4.0 \times 10^3$), 404 ($1.6 \times 10^3$). CD: $\lambda_{max}$, nm ($[\theta]_\lambda$, deg cm$^2$ dmol$^{-1}$) 600 (0), 425 (+9000), 395 (0), 347 (−8400).

**C. X-ray Data Collection and Processing.** Table 2 lists the color, habit, size, and solvent mixture from which each of the crystals was obtained. The crystal data and details of data collection are given in Table 3.

A suitable crystal of each compound was mounted on a glass fiber and placed on a Siemens P4 diffractometer. Intensity data were taken in the $\omega$ mode with graphite-monochromated Mo K$\alpha$ radiation ($\lambda = 0.710\,73$ Å). Two check reflections, monitored every 100 reflections, showed random (<2%) variation during the data collection. The data were corrected for absorption using a semiempirical model (maximum and minimum transmissionm factors are given in Table 3); this model was derived from an azimuthal data collection. Scattering factors and corrections for anomalous dispersion were taken from a standard source.[30] Calculations were performed with the Siemens SHELXTL Plus (version 5.0) software package on a PC. The structures were solved by Patterson methods. Anisotropic thermal parameters were assigned to non-hydrogen atoms where appropriate. Hydrogen atoms were refined at calculated positions with a riding model in which the C−H vector was fixed at 0.96 Å. The data were refined by the method of full-matrix least squares on $F^2$. Final cycles of refinement gave the $R(F)$ and $R_w(F)$ values presented in Table 3, where $w^{-1} = \sigma^2F + 0.001F^2$. Absolute configurations were determined by refinements of the Flack[31] parameters. The known absolute configuration at the benzylic carbon atom of each of the two diastereomers in the starting chloro compounds **1a,a′** and **1b,b′** also served as an internal reference in verifying[15] the absolute configuration at the Ru(II) center in each of the products.

**Acknowledgment.** We thank Professor David A. Lightner for his generous permission to use the Jasco spectropolarimeter, Dr. Stephan Boidjiev for helpful discussions on CD techniques and spectra, Professor Kenneth M. Doxsee for his gift of 1,3,4-triphenyl-1,2-dihydrophosphete, and a reviewer for the suggestion of the dissociative reaction mechanism. We are grateful to the donors of the Petroleum Research Fund (administered by the American Chemical Society) for financial support, to Johnson Mathey Aesar/Alfa for a generous loan of $RuCl_3 \cdot 3H_2O$, and to the National Science Foundation (Grant No. CHE-9214294) for funds to purchase the 500 MHz NMR spectrometer.

**Supporting Information Available:** For **3a**, **4b′**, **5a**, **6aa′**, **6a**, **13(*RS*)a**, **14b′**, and **15a**, tables of X-ray crystallographic data including crystallographic data, atomic coordinates, hydrogen atom coordinates, anisotropic thermal parameters, and interatomic distances and angles (66 pages). Ordering information is given on any current masthead page.

OM960064B

(30) *International Tables for X-ray Crystallography*; D. Reidel: Boston, MA, 1992; Vol. C.

(31) Flack, H. D. *Acta Crystallogr.* **1983**, *A39*, 876.